VIBRATION AND STABILITY OF COMPOSITE PANELS WITH GEOMETRICAL DISCONTINUITIES

SATISH KURMA
Roll No.: 211CE2026

Department of Civil Engineering
National Institute of Technology, Rourkela
Rourkela-769 008, Odisha, India

VIBRATION AND STABILITY OF COMPOSITE PANELS WITH GEOMETRICAL DISCONTINUITIES

A THESIS SUBMITTED IN PARTIAL FULFILMENT
OF THE REQUIREMENTS FOR THE DEGREE OF

Master of Technology

in

Structural Engineering

by

SATISH KURMA

(Roll No. 211CE2026)

DEPARTMENT OF CIVIL ENGINEERING
NATIONAL INSTITUTE OF TECHNOLOGY, ROURKELA
ROURKELA – 769 008, ODISHA, INDIA

VIBRATION AND STABILITY OF COMPOSITE PANELS WITH GEOMETRICAL DISCONTINUITIES

A THESIS SUBMITTED IN PARTIAL FULFILMENT
OF THE REQUIREMENTS FOR THE DEGREE OF

Master of Technology

in

Structural Engineering

by

SATISH KURMA

Under the guidance of

Prof. S.K. SAHU

DEPARTMENT OF CIVIL ENGINEERING
NATIONAL INSTITUTE OF TECHNOLOGY, ROURKELA
ROURKELA – 769 008, ODISHA, INDIA

MAY 2013

Department of Civil Engineering
National Institute of Technology, Rourkela
Rourkela – 769 008, Odisha, India

CERTIFICATE

This is to certify that the thesis entitled, ***"VIBRATION AND STABILITY OF COMPOSITE PANELS WITH GEOMETRICAL DISCONTINUITIES"*** *submitted by* ***SATISH KURMA*** *bearing Roll No.* ***211CE2026*** *in partial fulfilment of the requirements for the award of* ***Master of Technology*** *Degree in* ***Civil Engineering*** *with specialization in* ***"Structural Engineering"*** *at National Institute of Technology, Rourkela is an authentic work carried out by him under my supervision and guidance.*

To the best of my knowledge, the matter embodied in the thesis has not been submitted to any other University/Institute for the award of any Degree or Diploma.

Date:
Place: Rourkela

Prof. S.K.SAHU

ACKNOWLEDGEMENTS

The satisfaction and euphoria on the successful completion of any task would be incomplete without the mention of the people who made it possible whose constant guidance and encouragement crowned out effort with success.

I would like to express my heartfelt gratitude to my esteemed supervisor, **Prof. S. K. Sahu** for his technical guidance, valuable suggestions, and encouragement throughout the year in preparing this thesis. It has been an honour to work under Prof. S. K. Sahu , whose expertise and discernment were key in the completion of this project.

I am grateful to the **Department of Civil Engineering, NIT Rourkela,** for giving me an opportunity to execute this project, which is an integral part of the curriculum in M.Tech programme at the National Institute of Technology, Rourkela.

Many thanks to all my friends, who are directly or indirectly, helped me in my project work for their generous contribution towards enriching the quality of the work.

This acknowledgement would not be complete without expressing my sincere gratitude to my parents for their love, patience, encouragement, and understanding which are the source of my motivation and inspiration throughout my work.

SATISH KURMA

ABSTRACT

Laminated composite panels are becoming the preferred material system in a variety of industrial applications, such as aerospace vehicles, automotive structural parts and civil engineering structures for design and strengthening of concrete members. The present study deals with the numerical investigations on free vibration and buckling of composite panels with geometric non linearity such as Delamination and Cutout. A composite panel model based on first order shear deformation theory (FSDT) with provision of cut out and mid plane delamination is considered for the study of vibration and stability, in which stability is carried out only for cutout. The parametric study on composite panels showing the effect of percentage delamination and percentage cutout, aspect ratio, Number of layer, boundary conditions on Natural Frequency and buckling load has been studied. The basic understanding of the influence of the delamination and cutout on the natural frequencies and buckling load of composite panels is presented. In addition, other factors affecting the vibration and buckling region of delaminated composite plates and shells are discussed. The results indicate that the vibration and buckling behaviour is greatly influenced by the geometrical discontinuities.

TABLE OF CONTENTS

LIST OF FIGURES

LIST OF TABLES

LIST OF SYMBOLS

SYMBOLS FOR DELAMINATION FORMULATION

a,b	Plate dimensions along x- and y-axes, respectively
[K]	bending stiffness matrix
[Kg]	geometric stiffness matrix
ω	natural frequency
[M]	mass matrix
{∅}	eigenvectors i.e. mode shape
P	buckling load
P_{cr}	critical buckling load.
θ	Fibre orientation in a lamina
x ,y ,z	System of coordinate axes
t	thickness of plate
u, v, w	Displacement along x, y and z direction
Nx, Ny, Nxy	In-plane internal force resultants per unit length
Z_k, Z_{k-I}	Top and bottom distances of a lamina from the mid-plane
Ni	Shape function at a node i
Kx, Ky, Kxy	Curvatures of a plate
Mx, My, Mxy	Internal moment resultants per unit length
G_{l2}, G_{13}, G_{23}	Shear moduli of a lamina with respect to 1, 2, and 3 axes
E_1, E_2	Young's moduli of a lamina along and across fibres, respectively
Qx, Qy	Transverse shear resultants per unit length

SYMBOLS FOR CUTOUT FORMULATION

a, b	Length and width of the plate
ca, cb	Length and width of the cutout
A/h	Amplitude ratio
$\{e\}^L$	Linear strain vector
$\{e\}^{NL}$	Non-linear strain vector
e_p , e_b , e_s	Membrane, bending and shear strains
e*, e_s	Higher order bending and shear strains
[NA]	Linear stiffness matrix
[NB], [NC]	Non-linear stiffness matrices
[NS]	Linear stiffness matrix (shear)
UMB	Membrane and bending strain energy
US	Shear strain energy
[d]	Displacement gradient vector
[ds]	Drift Limit
$\{\delta\}$	Generalized displacement vector
NL	Equivalent Viscous damping
e	Subscript for the element
ω	Natural frequency
ω_{1NL}	Fundamental non-linear frequency
T	Kinetic energy
[M]	Mass matrix
$[K]^L$	Linear stiffness matrix
W	Weight of the plate

mc	Material code
P_c	Probability of crossover
P_m	Probability of mutation

CHAPTER 1

INTRODUCTION

1.1 OVERVIEW

A composite material can be defined as a mixture of two or more materials that results in better qualities than those of the individual material used alone. Over the last thirty years composite materials have been the dominant emerging materials. The volume and number of applications of composite materials have grown steadily, penetrating and conquering new markets relentlessly. Modern composite materials constitute a significant proportion of the engineered materials market ranging from everyday products to sophisticated niche applications. The main advantages of composite materials are their high strength and stiffness, combined with low density, when compared with bulky materials, allowing weight reduction in the finished part.

Composite panels may have a lot of geometrical discontinuities which may be in the form of delamination or in the form of cutout. Damages and flaws take a complex form, and alter their mechanical characteristics and behaviour. Delamination is inevitable as they are caused by some manmade activities like dropping of tools or bird hit. Delamination is one of the most severe defects associated with composite structures as it progresses or it may extend gradually to reduce the effective stiffness of the laminate.

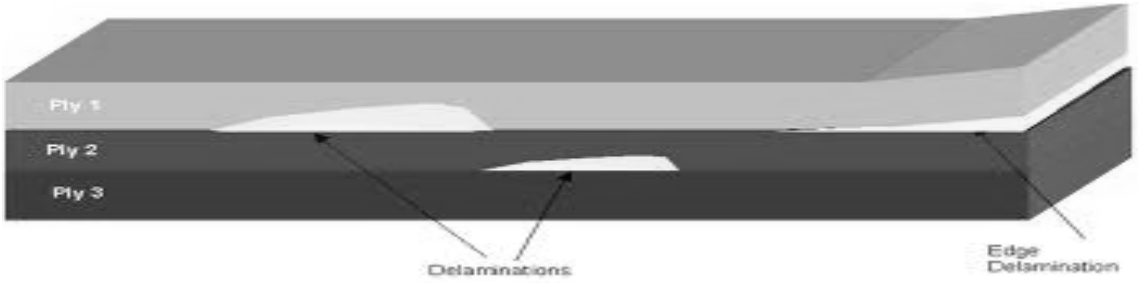

Figure 1.1: Typical Example of Composite Plate with Delamination

The cutouts are provided for reducing the weight, for accommodating fuel, hydraulic or for accommodating electrical lines and for providing accessibility to other parts of structures. Cutouts are inevitable in structures. Composite plates consisting of cutouts are extensively used in aerospace structures. The presence of a cutout reduces the stiffness and inertia of the composite spherical shell cap, thereby affecting the natural frequencies.

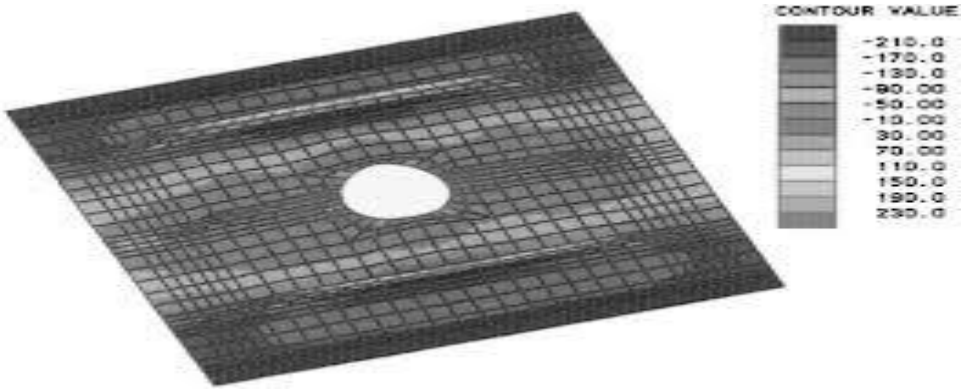

Figure 1.2: Typical Example of Composite Plate with Cutout

1.2 IMPORTANCE OF PRESENT STUDY

If the effect of the geometrical discontinuities can be accurately predicted, changes in modal dynamic characteristics could be used to determine the location and extent of delamination and cutout in composite structures. This information would be useful in non-destructive evaluation during manufacturing and for life prediction of composite parts in service or can be useful for structural health monitoring.

The importance of the present study is due to following advantages and applications of composites.

1. Tensile strength of composites is four to six times greater than that of steel or aluminium.
2. Improved torsional stiffness and impact properties.

3. Higher fatigue endurance limit (up to 60% of the ultimate tensile strength).
4. 30-45% lighter than aluminium structures designed to the same functional requirements
5. Lower embedded energy compared to other structural materials like steel, aluminium etc.
6. Composites are less noisy while in operation and provide lower vibration transmission than metals
7. Composites are more versatile than metals and can be tailored to meet performance needs and complex design requirements
8. Long life offers excellent fatigue, impact, environmental resistance and reduced maintenance
9. Composites enjoy reduced life cycle cost compared to metals.
10. Composites exhibit excellent corrosion resistance and fire retardancy.
11. Improved appearance with smooth surfaces and readily incorporable integral decorative melamine are other characteristics of composites
12. Composite parts can eliminate joints/fasteners, providing part simplification and integrated design compared to conventional metallic parts

1.3 OBJECTIVE AND SCOPE OF PRESENT STUDY

To study the effects of different parameters like percentage of delamination, size of cutouts, aspect ratio, ply orientation, number of layers and effect of curvature on the vibration and stability of composite panels subjected to geometrical discontinuities.

1.4 OUTLINE OF THE PRESENT STUDY-

In the current investigation the main objective is to find out the free vibration of composite panels with delamination, cutout and buckling analysis of a composite plate with cut out numerically by using softwares like MATLAB, ABAQUS CAE. Natural frequencies and buckling load are obtained for composite panels having geometrical discontinuities (like delamination and cutout) and parametric studies have been carried out by varying different parameters.

CHAPTER 2

LITERATURE REVIEW

2.1 OVERVIEW

Composite panels find widespread applications in many engineering fields namely aerospace, civil, biomedical, marine and mechanical engineering. Fibre reinforced composites are used extensively in the form of relatively thin plate as they have good strength to stiffness ratio and weight to stiffness ratio. They also possess excellent damage tolerance and impact resistance. Due to vibration and buckling, the composite panels are subjected to geometrical discontinuities such as delamination and cutout. In this chapter, the literature review has been done to show the amount of work carried out in the field vibration and buckling of composite curved panels with delamination and cutout.

2.2 VIBRATION OF COMPOSITE PANELS WITH DELAMINATION

Tenek et al. (1993) studied the vibration of delaminated composite plates and found out the impact of delamination on the natural frequencies of composite plates, as well as delamination dynamics over a broad frequency range, by using the finite element method based on the three-dimensional theory of linear elasticity. They have compared the method with experimental observations for the case of cantilever graphite-epoxy laminated plates.

Lee et al. (1995) investigated the free vibration of composite plates with delamination around cutouts and presented a finite element approach to analyze the free vibration of square and circular composite plates with delamination around internal cutouts for simply supported boundary conditions. They carried out Numerical analysis and discussed the effects of the cutouts and the delamination's around the cutouts on the natural frequencies and mode shapes.

Campanelli and Engblom (1995) observed the effect of delaminations in graphite/Polyetheretherketone(PEEK) composite plates on modal dynamic characteristics by using experimental and analytical studies. In this study they developed a computationally efficient 'plate type' finite element model to accurately predict the effect of delamination's on the modal dynamic characteristics of a laminated composite plate with simply supported boundary conditions.

Lee et al.(1995) conducted free vibration of delaminated composite plates with arbitrary boundary conditions, using finite element formulation based on Mindlin plate theory, with multiple delamination's and investigated the effects of boundary conditions, delamination size, delamination location and the number of delamination's on the natural frequencies and mode shapes of delaminated composite plates by using Numerical studies.

Chang et al.(1998) performed the vibration analysis of delaminated composite plates under axial load and introduced the concept of continuous analysis, which is proposed by Wang(1995) , to model the delaminated composite plate as a plate on a discontinuous elastic foundation by conducting Numerical studies. They represented the elastic adhesive layer between the buckled composite plate and the undeformed substructure working as a foundation to the plate, subjected to simply supported boundary conditions, by linear parallel springs.

Williams et al.(1998) presented a Numerical studies on dynamic model for graphite-epoxy laminated plates with delaminations and developed a generalized theory by using a finite element method for laminated as well as delaminated plates. They proposed a theory that imposes no restrictions on the size, location, distribution, or direction of growth of the delamination's. and also considered the influence of the delamination on the free vibration behavior of a plate.

Geubella and Baylor (1998) studied a 2D simulation of Impact-induced delamination of graphite/epoxy composites plates by using an analytical method. They simulated the delamination process in thin cantilever composite plates subjected to low-velocity impact by using a specially developed 2D cohesive/volumetric finite element scheme. They considered the simulation as dynamic and used an explicit time stepping scheme.

Hou and Jeronimidis (1999) performed the analytical and experimental studies on vibration of delaminated composite plates with free- free boundary conditions and conducted free vibration tests on E-glass/Epoxy composite plates by using finite element model to study the effect of low-velocity impact induced damage consisting of inter laminar delamination accompanied by matrix cracking on the natural frequencies of thin composite laminated circular plates.

Parhi et al (2000) performed the finite element dynamic analysis of carbon epoxy laminated composite plates with multiple delaminations' located in arbitrary position. They presented the numerical results for free vibration and transient response for single and multiple delaminated composite plates with various boundary conditions, stacking sequences and other geometric parameters.

Ostachowicz and Kaczmarezyk (2001) investigated the vibration of composite plates with shape memory alloys fibers by using a Numerical finite element model in a gas stream with defects of the type of delamination and analyzed the dynamics of multi layer composite plate with delamination's subjected to an aero dynamic load and simply supported boundary conditions. They also studied the effect of delamination on the natural frequencies of the plate subjected to supersonic flow and determined the flutter instability boundaries.

Hu et al.(2002) presented vibration analysis of delaminated composite beams and plates using a higher-order finite element theory by considering various boundary condition. They

analyzed the vibration response of delaminated composite plates of moderate thickness, which can satisfy the zero transverse shear strain condition on the top and bottom surfaces of plates and also investigated the influences of delamination on the vibration characteristic of composite laminates by using analytical model.

Chen et al. (2004) investigated the dynamic response behavior of delaminated plates by considering progressive failure process of modified Newmark direct integral method in conjunction with Tsai's failure criteria. They discussed the effects of frequency of dynamic load, delamination length and location, and reduction of structure stiffness during the progressive failure process upon dynamic behavior of the delaminated composite plates with simply supported boundary conditions by some numerical studies.

Yam et al. (2004) proposed a three-dimensional finite element model for the delaminated fiber reinforced composites to carry out the numerical analysis of multi-layer composite plates with internal delamination. They analyzed the natural frequency, modal displacement and modal strain for samples with different dimensions of delamination and by using free boundary conditions on all sides.

Oh et al. (2005) carried out numerical analysis on the dynamic analysis of graphite-epoxy composite plate with multiple delamination's based on higher-order zigzag theory. They developed a four-node finite element model to refine the prediction of frequencies, mode shape, and time response with cantilever boundary conditions.

2.3 VIBRATION OF COMPOSITE PANEL WITH CUTOUT

Lee et al. (1987) performed numerical analysis based on ray leigh ritz method for predicting the natural frequencies of graphite epoxy rectangular composite plates for simply supported boundary condition having central rectangular cutouts and double square cutouts using finite element method.

Sivakumar K (1998) investigated free vibration analysis of graphite epoxy isotropic composite plates using finite element analysis. He obtained results for different cutout shapes such as square, rectangle, circle and ellipse subjected to various boundary conditions and aspect ratios.

Sai ram et al. (2002) studied **t**he free vibration of composite spherical shell cap with and without cutout. The analysis is carried out using the finite element method based on a higher-order shear deformation theory. Results are presented for axisymmetric free vibration of composite spherical shell cap with and without a cutout. The effects of number of plies, radius to thickness ratio, boundary conditions and cutout size on the fundamental frequency of orthotropic and laminated composite spherical shell cap are also presented.

Namita et al. (2007) carried out nonlinear free vibration of laminated composite cylindrical shell panels in the presence of cutouts. They used finite element method for the parametric study by varying the aspect ratios, lamination schemes and material properties of cylindrical shell with simply supported boundary condition in the presence of cutouts.

Pandit et al. (2007) used a nine-noded isoparametric plate-bending element to perform the analysis of free undamped vibration of isotropic and fiber reinforced laminated composite plates. The effect of shear deformation has been incorporated in the formulation by considering the first-order shear deformation theory for the analysis.

Sasank et al. (2007) studied the vibration analysis of isotropic plates numerically with arbitrary shaped cutouts subjected to simply supported and clamped boundary conditions, using finite element method.

Poore A.L et al. (2008) studied the free vibration of laminated cylindrical shells with a circular cutout subjected to simply supported boundary conditions using a semi analytical solution and also investigated the effect of increasing the cutout size, effect of fiber

orientation, effect of cutout with increasing shell radius and effect of cutout with increasing plies.

2.4 BUCKLING OF COMPOSITE PANEL WITH CUTOUT

Giulio (2001) studied the behaviour of laminated panels with rectangular opening under biaxial tension, compression and shear loads analytically and experimentally. Finite Element Method was carried out to find the buckling behaviour of panels and it is compared with experimental results. The study was conducted on graphite epoxy composite plates.

Murat et al. (2003) performed finite element analysis to predict the effects of cut-outs on the buckling behaviour of composite plates reinforced with glass fibers. He studied the effects of cut-out size, cut-out orientation and corner fillet radius conditions by both numerically and experimentally.

Payal Jain et al. (2004) investigated the post buckling response of symmetric square laminates with a central cutout under uniaxial compression using finite element method.

Ghannadpour et al. (2006) studied the effects of a cutout on the buckling behaviour of rectangular plates made of polymer matrix composites (PMC) by numerical method. The study is concentrated on the behaviour of rectangular symmetric cross-ply laminates subjected to clamped and simply supported boundary condition using Finite element analysis.

Hamit et al. (2007) investigated the buckling behaviour of simply supported composite laminated square plates with corner circular notches under in-plane static loadings are investigated using the first- order shear deformation theory (FSDT) with a Fortran computer code. Finite element method (FEM) is also used to predict the effects of notch sizes, plate thickness ratios, material modulus ratios, loadings, various reinforcement angles, and ply lamination geometry on the critical buckling loads.

Aydin et al. (2010) carried out buckling analysis on woven–glass–polyester laminated composite plate numerically with a circular/elliptical hole using finite element method. He studied the effect of increase of cutout on buckling load for a plate subjected to CFCF boundary condition using finite element method.

Dinesh Kumar et al. (2010) studied the effects of flexural boundary conditions on buckling and post buckling behaviour of axially compressed quasi-isotropic laminate with various shaped cutouts (i.e., circular, square, diamond, elliptical–vertical and elliptical–horizontal) numerically for various sizes using the finite element method based on first order shear deformation theory.

2.5 SUMMARY

Based on the critical assessment of literature, it can be conclude that geometrical discontinuities like delamination and cutout having a significant effect on vibration and buckling of composite panels. There are only very few number of research works are available in the field of parametric studies on geometrical discontinuities of composite panels.

CHAPTER 3

MATHEMATICAL FORMULATION

3.1 GENERAL

This chapter describes the finite element mathematical formulation for vibration and stability analysis of the composite panels with geometrical discontinuities.

3.2 COMPOSITE PANELS WITH DELAMINATION

The basic configuration of the problem considered here is a doubly curved panel with mid plane single delamination subjected to in plane periodic load. The boundary conditions are incorporated in the most general manner.

3.2.1. Proposed Analysis

The governing equations for the vibration and stability of the delaminated composite panels are derived on the basis of first order shear deformation theory. The element stiffness, geometric stiffness and mass matrices are derived on the basis of principle of minimum potential energy and Lagrange's equation.

3.2.2 Governing Equation for Analysis

Equation for free vibration is,

$$\left([K]-\omega^2[M]\right)\{\phi\}=\{0\}$$

Where $[K]$ and $[M]$ are the global stiffness and global mass matrices, $\{\phi\}$ is the natural frequency and is the corresponding eigenvectors i.e. mode shape.

Equation for buckling analysis is**,**

$$\left([K]-P[K_g]\right)\{\phi\}=\{0\}$$

Where,

$[K]$ and $[K]_g$ are the bending stiffness matrix and geometric stiffness matrix. The Eigen values of the above equation gives the buckling loads for different modes. The lowest value of buckling load (P) is termed as critical buckling load (P_{cr}) of the structure.

M, K and K_G are the mass, the stiffness and the geometric matrices.

3.2.3 Finite Element Analysis

A laminated doubly curved shell panel of length *a*, width *b* and thickness *h* consisting of n arbitrary number of anisotropic layers is considered as shown in Figure 3.1. The layer details of the laminate are shown in Figure 3.2. The displacement field is related to mid-plane displacements and rotations as

$$u(x,y,z,t) = u^0(x,y,z,t) + z\,\theta_x(x,y,t)$$

$$v(x,y,z,t) = v^0(x,y,z,t) + z\,\theta y(x,y,t)$$

$$w(x,y,z,t) = w^0(x,y,z,t)$$

Where *u*, *v* and *w* are displacements in *x*, *y* and *z* directions, respectively, and the superscript (0) corresponds to the mid-plane values. Here, θ_x and θ_y denote the rotations of the cross sections perpendicular to the *y*- and *x*-axis respectively.

Using Sander's first approximation theory for thin shells, the generalized strains in terms of mid-plane strains and curvatures are expressed as

$$\{\varepsilon_{xx} \quad \varepsilon_{yy} \quad \gamma_{xy} \quad \gamma_{xz} \quad \gamma_{yz}\}^T = \{\varepsilon^0_{xx} \quad \varepsilon^0_{yy} \quad \gamma^0_{xy} \quad \gamma^0_{xz} \quad \gamma^0_{yz}\}^T + \{k_{xx} \quad k_{yy} \quad k_{xy} \quad k_{xz} \quad k_{yz}\}^T$$

Where,

$$\begin{Bmatrix} \varepsilon_{xx}^0 \\ \varepsilon_{yy}^0 \\ \gamma_{xy}^0 \\ \gamma_{xz}^0 \\ \gamma_{yz}^0 \end{Bmatrix} = \begin{Bmatrix} \dfrac{\partial u}{\partial x} + \dfrac{\omega}{R_x} \\ \dfrac{\partial v}{\partial x} + \dfrac{\omega}{R_y} \\ \dfrac{\partial u}{\partial y} + \dfrac{\partial v}{\partial x} + \dfrac{\omega}{R_{xy}} \\ \theta_x + \dfrac{\partial \omega}{\partial x} \\ \theta_y + \dfrac{\partial \omega}{\partial y} \end{Bmatrix}$$

and

$$\begin{Bmatrix} k_{xx} \\ k_{yy} \\ k_{xy} \\ k_{xz} \\ k_{yz} \end{Bmatrix} = \begin{Bmatrix} \dfrac{\partial \theta_x}{\partial x} \\ \dfrac{\partial \theta_y}{\partial x} \\ \dfrac{\partial \theta_x}{\partial x} + \dfrac{\partial \theta_y}{\partial y} \\ 0 \\ 0 \end{Bmatrix}$$

And R_x, R_y and R_{xy} are the three radii of curvature of the shell element. The entire dynamic Equations of equilibrium reduce to that for the plate, when the values of R_x, R_y, and R_{xy} become ∞. The five degrees of freedom considered at each node of the element are u^0, v^0, w, θ_x and θ_y. By using the eight-noded element shape functions, the element displacements are expressed in terms of their nodal values given by

$$u^0 = \sum_{i=1}^{8} N_i u_i^0 \;\; v^0 = \sum_{i=1}^{8} N_i v_i^0 \;\; \omega^0 = \sum_{i=1}^{8} N_i \omega_i^0$$

$$\theta_x = \sum_{i=1}^{8} N_i \theta_{xi} \;\; \theta_y = \sum_{i=1}^{8} N_i \theta_{yi}$$

Where N_i 's are the shape functions used to interpolate the generalized displacements $u_i^0, v_i^0, \omega_i, \theta_{xi}, \theta_{yi}$, and at node *i* within an element.

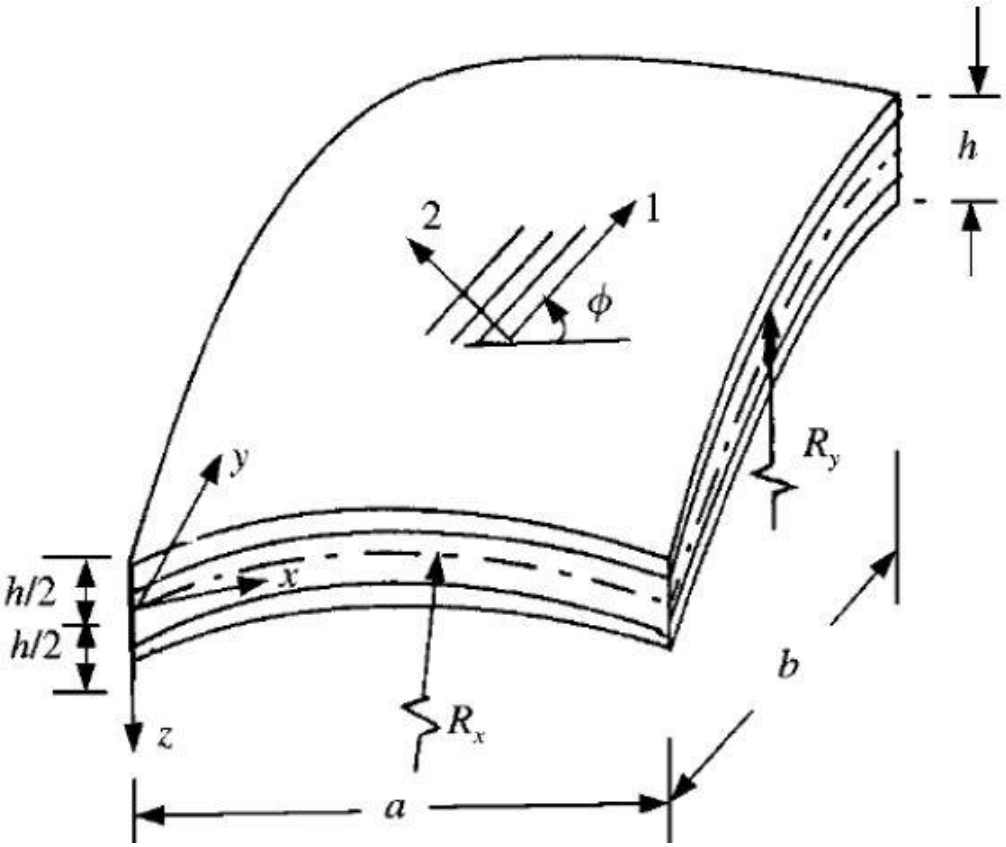

Figure 3.1: Laminated composite doubly curved axis

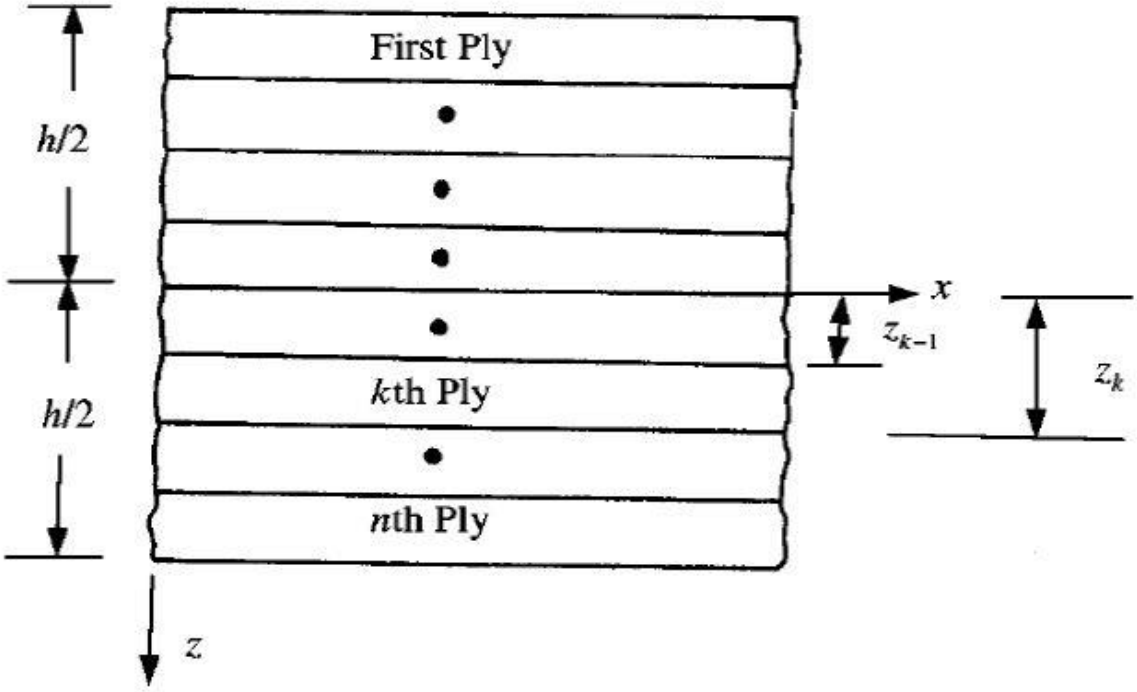

Figure 3.2:. Layer details of shell panel.

The stress resultants are related to the mid-plane strains and curvatures for a general laminated shell element as

$$\begin{Bmatrix} N_x \\ N_y \\ N_{xy} \\ M_x \\ M_y \\ M_{xy} \\ Q_y \\ Q_x \end{Bmatrix} = \begin{bmatrix} A_{11} & A_{12} & A_{16} & B_{11} & B_{12} & B_{16} & & \\ A_{12} & A_{22} & A_{26} & B_{12} & B_{22} & B_{26} & & \\ A_{16} & A_{26} & A_{66} & B_{16} & B_{26} & B_{66} & & \\ B_{11} & B_{26} & B_{16} & D_{11} & D_{12} & D_{16} & & \\ B_{12} & B_{22} & B_{26} & D_{12} & D_{22} & D_{26} & & \\ B_{16} & B_{26} & B_{66} & D_{16} & D_{26} & D_{66} & & \\ & & & & & & A_{44} & A_{45} \\ & & & & & & A_{45} & A_{55} \end{bmatrix} = \begin{Bmatrix} \varepsilon_{xx}^0 \\ \varepsilon_{yy}^0 \\ \gamma_{xy}^0 \\ K_{xx} \\ K_{yy} \\ K_{xy} \\ \gamma_{yz}^0 \\ \gamma_{xz}^0 \end{Bmatrix}$$

Where $N_x, N_y\ N_x$, and are in-plane stress resultants, and $M_x\ M_y\ M_{xy}$ are moment resultants and Q_x, Q_y are transverse shear stress resultants. The extensional, bending-stretching and bending stiffness's of the laminate are expressed in the usual form as

$$(Aij, Bij, Dij) = \sum_{k=1}^{n} \int_{x_{k-1}}^{x_k} (Q_{ij})_k \, (1, z, z2)dz, \; i, j = 1, 2, 6.$$

Similarly, the shear stiffness is expressed as

$$(Aij) = \sum_{k=1}^{n} \int_{x_{k-1}}^{x_k} \alpha (Q_{ij})_k \, dz \; i, j = 4,5$$

α is the shear correction factor which is derived from the Timoshenko beam concept by applying the energy principle is assumed as 5/6. It accounts for the non-uniform distribution of transverse shear strain across the thickness of the laminate.

$(\bar{\bar{Q}}_{ij})_k$ are off-axis stiffness values defined as

$$(\bar{\bar{Q}}_{ij})_k = \begin{bmatrix} m^2 & n^2 & -2mn \\ n^2 & m^2 & -mn \\ mn & -mn & m^2 - n^2 \end{bmatrix} (Q_{ij})_k \begin{bmatrix} m^2 & n^2 & mn \\ n^2 & m^2 & -mn \\ -2mn & 2mn & m^2 - n^2 \end{bmatrix} \quad i,j=1,2,6$$

$$(\bar{\bar{Q}}_{ij})_k = \begin{bmatrix} m & -n \\ n & m \end{bmatrix} (Q_{ij})_k \begin{bmatrix} m & n \\ -n & m \end{bmatrix} I,j=4,5$$

Where, m=cosθ, n=sinθ

$(Q_{ij})_k$ are calculated in the conventional manner from the values of elastic and shear moduli and the Poisson ratio values.

$$Q_{11} = E_1/(1-\upsilon_{12}\upsilon_{21}) \; , \; Q_{12} = \upsilon_{12}E_2/(1-\upsilon_{12}\upsilon_{21}), \; Q_{21} = \upsilon_{12} \, E_2/(1-\upsilon_{12}\upsilon_{21}) \; , \; Q_{22} = E_2/(1-\upsilon_{12}\upsilon_{21})$$

$$Q_{66}= G_{12}, \; Q_{44}= G_{13}, \; Q_{55}= G_{23}.$$

Where,

E_1, E_2 = Young‟s moduli of a lamina along and across the fibres, respectively

G_{12}, G_{13}, G_{23} = Shear moduli of a lamina with respect to 1,2 and 3 axes.

υ_{12}, $\upsilon 21$= Poisson's ratios.

The element stiffness matrix, [Ke] is given by

$$[K_e] = \int_{-1}^{1} \int_{-1}^{1} [B]^T [D][B] J d\xi d\eta$$

Where,

[B] is stain-displacement matrix

[D] is the elasticity matrix

J is the Jacobean

Full integration (3x3) is used for bending stiffness, whereas reduced integration (2x2) is employed to evaluate transverse stiffness of the elements. A 2 point integration eliminates the shear locking in case of thin plates.

Similarly the consistent element mass matrix [Me] is expressed as

$$[M_e] = \int_{-1}^{1} \int_{-1}^{1} [N]^T [\rho][N] J d\xi d\eta$$

With [N], the shape function matrix and [ρ], the inertia matrix. The element load vector,{Fe} is presented by

$$[M_e] = \int_{-1}^{1} \int_{-1}^{1} [N]^T [\rho][N] J d\xi d\eta$$

Where {q} is the intensity of external transverse uniform loading.

The shape functions N_i are defined as

$N_i = (1+\xi\xi_i)(1+\eta\eta_i)(\xi\xi_i + \eta\eta_i - 1)/4$ i=1to4

$N_i = (1-\xi^2)(1+\eta\eta_i)/2$ i=5,7

$N_i = (1+\xi\xi_i)(1-\eta^2)/2$ i=6,8

Where ξ and η are the local natural coordinates of the element and ξi and η_i are the values at ith mode. The derivatives of the shape function N_i with respect to x, y are expressed in term of their derivatives with respect to ξ and η by the following relationship

$$\begin{bmatrix} N_{ix} \\ N_{iy} \end{bmatrix} = [j]^{-1} \begin{bmatrix} N_{i\xi} \\ N_{i\eta} \end{bmatrix}$$

Where ,

$$[J] = \begin{bmatrix} \frac{\partial x}{\partial \xi} & \frac{\partial y}{\partial \xi} \\ \frac{\partial x}{\partial \eta} & \frac{\partial y}{\partial \eta} \end{bmatrix}$$

3.2.4 Strain displacement Relations

Green-Lagrange‟s strain displacement is used throughout the structural analysis. The linear part of the strain is used to derive the elastic stiffness matrix and non-linear part of the strain is used to derive the geometrical stiffness matrix.

$$\{\varepsilon\} = \{\varepsilon_l\} + \{\varepsilon_{nl}\}$$

The linear strains are defined as

$$\varepsilon_{xl} = \frac{\partial u}{\partial x} + \frac{w}{R_x} + Zk_x$$

$$\varepsilon_{xl} = \frac{\partial u}{\partial y} + \frac{w}{Ry} + Zk_y$$

$$\gamma_{xyl} = \frac{\partial u}{\partial y} + \frac{\partial v}{\partial x} + \frac{2w}{R_{xy}} + Zk_{xy}$$

$$\gamma_{xz} = \frac{\partial u}{\partial z} + \frac{\partial w}{\partial x} - C_1 \frac{u}{R_x} - C_2 \frac{v}{R_{xy}}$$

$$\gamma_{yz} = \frac{\partial w}{\partial y} + \frac{\partial v}{\partial z} - \frac{v}{R_y} - C_1 \frac{u}{R_{xy}}$$

Where the bending strains k_j are expressed as

$$K_x = \frac{\partial \theta_x}{\partial x}$$

$$K_y = \frac{\partial \theta_y}{\partial y}$$

$$K_{xy} = \frac{\partial \theta_x}{\partial y} - \frac{\partial \theta_y}{\partial x} + \frac{1}{2} C_2 \left(\frac{1}{R_y} - \frac{1}{R_x} \right) \left(\frac{\partial v}{\partial x} - \frac{\partial u}{\partial y} \right)$$

And C_1 and C_2 are tracers by which the analysis can be reduced to that of shear deformable Love's first approximations and Donnell's theories.

Assuming that *w* does not vary with *z*, the non-linear strains of the shell are expressed as

$\varepsilon_{xnl} = [(u_{,x} + w/R_x)^2 + + (w_{,xu}/R_x)^2]/2,$

$\varepsilon_{ynl} = [(v_{,y} + w/R_y)^2 + + (w_{,y}v/R_y)^2]/2,$

$\gamma_{xynl} = [(u_{,x} + w/R_x)u_{,y} + v_{,x}(v_{,y} + w/R_y) + (w_{,x}u/R_x)\,(w_{,y}v/R_y)],$

$\gamma_{xznl} = [(u_{,x} + w/R_x)u_{,z} + v_{,y}v_{,z} + (w_{,x}u/R_x)\,w_{,z}],$

$\gamma_{yznl} = [(u_{,y} + w/R_y)u_{,z} + v_{,y}v_{,z} + (w_{,y}u/R_y)\,w_{,z}],$

$$\{\varepsilon\} = [B]\{d_e\}$$

$$\{d_e\} = \{u_1 v_1 w_1 \theta_{x1} \theta_{y1} u_2 v_2 \ldots\ldots\ldots u_8 v_8 w_8 \theta_{x8} \theta_{y8}\}^T$$

$$[B] = [[B_1]\ \ [B_2]\ \ [B_3]\ \ [B_4]\ \ [B_5]\ \ [B_6]\ \ [B_7]\ \ [B_8]]$$

$$[B_i]=\begin{bmatrix} \frac{\partial N_i}{\partial x} & 0 & \frac{N_i}{R_x} & 0 & 0 \\ 0 & \frac{\partial N_i}{\partial y} & \frac{N_i}{R_y} & 0 & 0 \\ \frac{\partial N_i}{\partial y} & \frac{\partial N_i}{\partial x} & 0 & 0 & 0 \\ 0 & 0 & 0 & \frac{\partial N_i}{\partial x} & 0 \\ 0 & 0 & 0 & 0 & \frac{\partial N_i}{\partial y} \\ 0 & 0 & 0 & \frac{\partial N_i}{\partial y} & \frac{\partial N_i}{\partial x} \\ 0 & 0 & \frac{\partial N_i}{\partial x} & N_i & 0 \\ 0 & 0 & \frac{\partial N_i}{\partial y} & 0 & N_i \end{bmatrix}$$

Generalised element mass matrix or consistent mass matrix:-

$$[M_e]=\int_{-1}^{1}\int_{-1}^{1}[N]^T[\rho][N]Jd\xi d\eta$$

Where the shape function matrix

$$[\mathrm{N}]=\begin{bmatrix} N_i & 0 & 0 & 0 & 0 \\ 0 & N_i & 0 & 0 & 0 \\ 0 & 0 & N_i & 0 & 0 \\ 0 & 0 & 0 & N_i & 0 \\ 0 & 0 & 0 & 0 & N_i \end{bmatrix}$$

$$[\mathrm{P}]=\begin{bmatrix} P_1 & 0 & 0 & P_2 & 0 \\ 0 & P_1 & 0 & 0 & P_2 \\ 0 & 0 & P_1 & 0 & 0 \\ P_2 & 0 & 0 & P_3 & 0 \\ 0 & P_2 & 0 & 0 & P_3 \end{bmatrix}$$

Where,

$$\begin{pmatrix} P_1 & P_2 & P_3 \end{pmatrix} = \sum_{k=1}^{n} \int_{z_{k-1}}^{z_k} (\rho)_k \, (1, z, z^2) \, dz$$

The element mass matrix can be expressed in local natural co-ordinate of the element as.

$$[M_e] = \int_{-1}^{1} \int_{-1}^{1} [N]^T [\rho][N] J d\xi d\eta$$

3.2.5 Geometric Stiffness Matrix:

The element geometric stiffness matrix is derived using the non-linear in-plane Green's strains. The strain energy due to initial stresses is

$$U_2 = \int_v [\sigma^0]^T \{\varepsilon_{nl}\} dv$$

Using non-linear strains, the strain energy can be written in matrix form as

$$U_2 = \frac{1}{2} \int_v [f]^T [S][f] dv$$

$$\{f\} = \begin{bmatrix} \frac{\partial u}{\partial x} & \frac{\partial u}{\partial y} & \frac{\partial v}{\partial x} & \frac{\partial v}{\partial y} & \frac{\partial w}{\partial x} & \frac{\partial w}{\partial y} & \frac{\partial \theta_x}{\partial x} & \frac{\partial \theta_x}{\partial y} & \frac{\partial \theta_y}{\partial x} & \frac{\partial \theta_y}{\partial y} \end{bmatrix}$$

$$[S] = \begin{bmatrix} s & 0 & 0 & 0 & 0 \\ 0 & s & 0 & 0 & 0 \\ 0 & 0 & s & 0 & 0 \\ 0 & 0 & 0 & s & 0 \\ 0 & 0 & 0 & 0 & s \end{bmatrix}$$

$$[s] = \begin{bmatrix} \sigma_x & \tau_{xy} \\ \tau_{xy} & \sigma_y \end{bmatrix} = \frac{1}{h} \begin{bmatrix} N_x & N_{xy} \\ N_{xy} & N_y \end{bmatrix}$$

The in-plane stress resultants N_x ,N_y, N_{xy} at each gauss point are obtained by applying uniaxial stress in x-direction and the geometric stiffness matrix is formed for these stress resultants.

$$[f]=[G][\delta_e]$$

The strain energy becomes

$$U_2=\frac{1}{2}\int_v\{\delta_e\}^T[G]^T[S][G]\{\delta_e\}dv=\frac{1}{2}\{\delta_e\}^T[K_g]\{\delta_e\}$$

$$[G]=\begin{bmatrix} N_{ix} & 0 & 0 & 0 & 0 \\ N_{ix} & 0 & 0 & 0 & 0 \\ 0 & N_{ix} & 0 & 0 & 0 \\ 0 & N_{ix} & 0 & 0 & 0 \\ -N_i/R_x & 0 & N_{ix} & 0 & 0 \\ 0 & -N_i/R_x & N_{ix} & 0 & 0 \\ 0 & 0 & 0 & N_{ix} & 0 \\ 0 & 0 & 0 & N_{ix} & 0 \\ 0 & 0 & 0 & 0 & N_{ix} \\ 0 & 0 & 0 & 0 & N_{ix} \end{bmatrix}$$

3.2.6 Multiple delamination modelling

Considering a typical composite laminate having p number of delamination is considered.

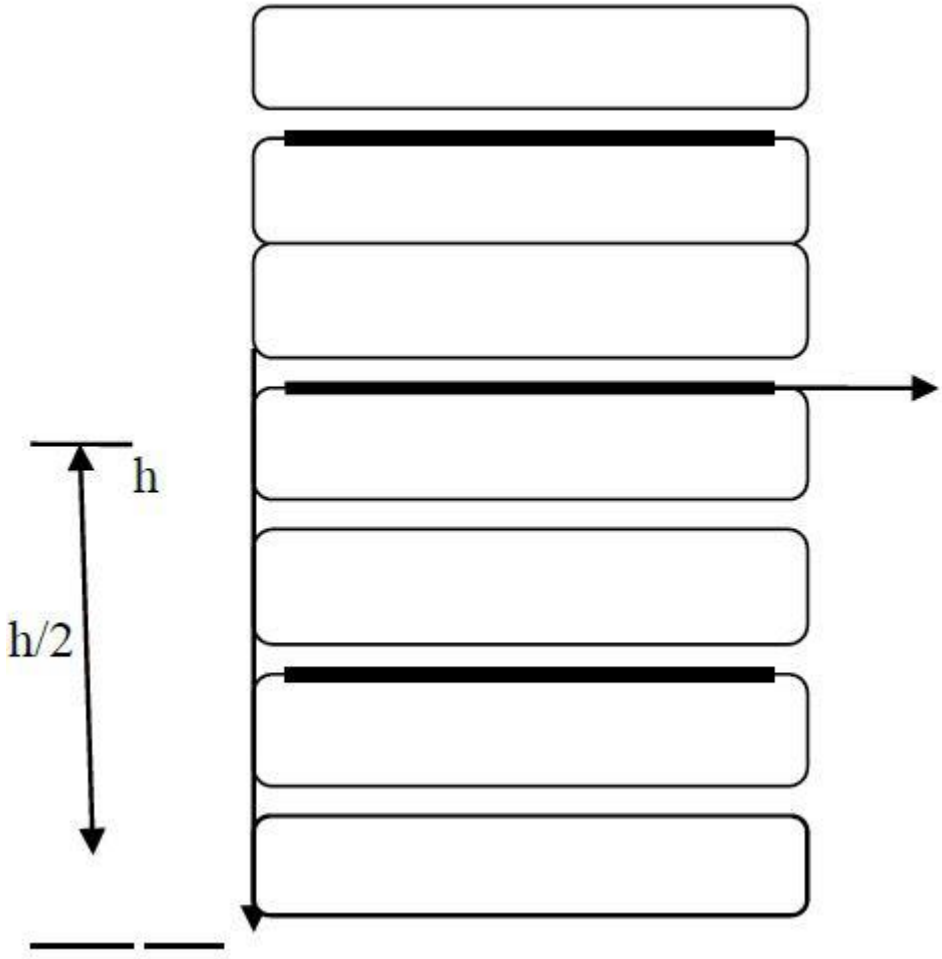

Figure 3.3: multiple model delamination.

$$u_t = u_t^0 + \left(z - z_t^0\right)\theta_{x,v_t} = v_t^0 + \left(z - z_t^0\right)\theta_{x,} \qquad (1)$$

Where u_t^0, v_t^0 are the mid-plane displacement of the t^{th}sub laminate and z_t^0, the distance between the mid-plane of the original laminate and the mid-plane of the t^{th}sub laminate. The strain component of any layer of a sub laminate are found from eqn (2) in the form of

$$\begin{Bmatrix} \varepsilon_{xx} \\ \varepsilon_{yy} \\ \gamma_{xy} \end{Bmatrix} = \begin{Bmatrix} \varepsilon_{xx}^0 \\ \varepsilon_{yy}^0 \\ \gamma_{xy}^0 \end{Bmatrix} + \left(z - z_t^0\right)\begin{Bmatrix} k_{xx} \\ k_{yy} \\ k_{xy} \end{Bmatrix} \qquad (2)$$

In the order to satisfy the compatibility condition at the delamination's boundary, it is assumed that transverse displacements and rotations at a common node for all the three sub laminates including the original one are identical. Applying this multipoint constraint condition, the midpoint displacements of any sub laminate t can be generalized as

$$u_t^0 = u^0 + z_t^0 \theta_{x,} v_t^0 = v^0 + z_t^0 \theta_{y,} \qquad (3)$$

The mid plane strain components of the t^{th} sub laminate are derived from it as

$$\begin{Bmatrix} \varepsilon_{xx} \\ \varepsilon_{yy} \\ \gamma_{xy} \end{Bmatrix} = \begin{Bmatrix} \varepsilon_{xx}^0 \\ \varepsilon_{yy}^0 \\ \gamma_{xy}^0 \end{Bmatrix} + \left(z_t^0\right) \begin{Bmatrix} k_{xx} \\ k_{yy} \\ k_{xy} \end{Bmatrix} \qquad (4)$$

Substituted eqn(4) into eqn(2),then we get strain components at any layer within a sub laminate. For any lamina of the t^{th} sub laminate, the in-plane and shear stresses are fined from the relations

$$\begin{Bmatrix} \sigma_{xx} \\ \sigma_{yy} \\ \tau_{xy} \end{Bmatrix} = \begin{bmatrix} \bar{\bar{Q}}_{11} & \bar{\bar{Q}}_{12} & \bar{\bar{Q}}_{16} \\ \bar{\bar{Q}}_{21} & \bar{\bar{Q}}_{22} & \bar{\bar{Q}}_{26} \\ \bar{\bar{Q}}_{16} & \bar{\bar{Q}}_{26} & \bar{\bar{Q}}_{66} \end{bmatrix} \begin{Bmatrix} \varepsilon_{xx} \\ \varepsilon_{yy} \\ \gamma_{xy} \end{Bmatrix}_t$$

$$\begin{Bmatrix} \tau_{xz} \\ \tau_{yx} \end{Bmatrix} = \begin{bmatrix} \bar{\bar{Q}}_{44} & \bar{\bar{Q}}_{45} \\ \bar{\bar{Q}}_{45} & \bar{\bar{Q}}_{55} \end{bmatrix} \begin{Bmatrix} \gamma_{xz} \\ \gamma_{yx} \end{Bmatrix}_t$$

Integrating these stresses over the thickness of the sub laminate, the stress and moment resultants of the sub laminate are desired which lend to the elasticity matrix of the t^{th} sub laminate is the form

$$[D]_t = \begin{bmatrix} A_{ij} & z_t^0 A_{ij} + B_{ij} & 0 \\ A_{ij} & z_t^0 B_{ij} + D_{ij} & 0 \\ 0 & 0 & S_{ij} \end{bmatrix}$$

Where

$$[A_{ij}]_t = \int_{\frac{-ht}{2}+Z_t^0}^{\frac{ht}{2}+Z_t^0} \left[\bar{\bar{Q}}_{ij}\right] dz$$

$$[B_{ij}]_t = \int_{\frac{-ht}{2}+Z_t^0}^{\frac{ht}{2}+Z_t^0} \left[\bar{\bar{Q}}_{ij}\right] (z - z_t^0) dz$$

$$[D_{ij}]_t = \int_{\frac{-ht}{2}+Z_t^0}^{\frac{ht}{2}+Z_t^0} \left[\bar{\bar{Q}}_{ij}\right] (z - z_t^0)^2 dz \text{ I,j=1,2,6}$$

$$[S_{ij}]_t = \int_{\frac{-ht}{2}+Z_t^0}^{\frac{ht}{2}+Z_t^0} \left[\bar{\bar{Q}}_{ij}\right] dz \text{ I,j=4,5}$$

Here h_t is the thickness of the t^{th} sub laminate.

3.3 COMPOSITE PANELS WITH CUTOUT

The problem is formulated for a plate of thickness h composed of orthotropic layers of thickness h_i with fibers oriented at angles θ, as shown in Figure 1. The higher-order displacement model which gives parabolic variation of shear stresses across the thickness of the laminate.

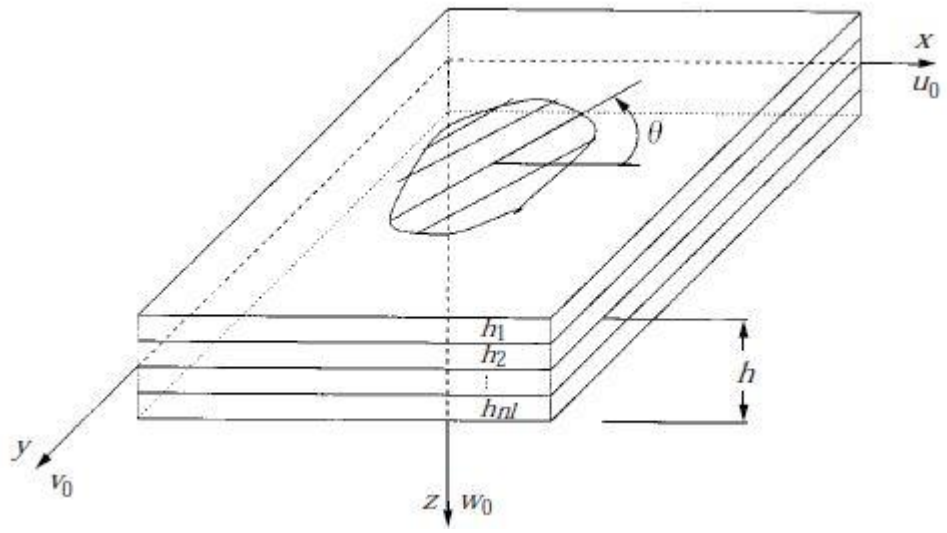

Figure 3.4. Laminated plate with co-ordinates and displacements

$$\begin{aligned} u(x,y,z;t) &= u_0(x,y,t) + f_1(z)\psi_x(x,y,t) + f_2(z)\theta_x(x,y,t), \\ v(x,y,z;t) &= v_0(x,y,t) + f_1(z)\psi_y(x,y,t) + f_2(z)\theta_y(x,y,t) \\ w(x,y,z;t) &= w_0(x,y,t), \end{aligned} \tag{1}$$

Where

$$f_1(z) = C_1 z - C_2 z^3, \; f_2(z) = -C_4 z^3 \tag{2,3}$$

with C_1=1, and C_2=C_4=4/3h2, u, v and w are the displacements along the x, y and z directions. u_0 , v_0 and w_0 are displacements of the middle plane of the laminate and θ_x, θ_y , ψ_x and ψ_y are the rotations and slope respectively along the x and y axes.

From the Green's strain vector, the non-linear strain displacement relation

$$\begin{Bmatrix} \varepsilon_x \\ \varepsilon_y \\ \gamma_{xy} \\ \gamma_{xz} \\ \gamma_{yz} \end{Bmatrix} = \begin{Bmatrix} u_{,x} + \frac{1}{2}(u_{,x}^2 + \frac{1}{2}v_{,x}^2 + \frac{1}{2}w_{,x}^2) \\ v_{,y} + \frac{1}{2}(u_{,y}^2 + \frac{1}{2}v_{,y}^2 + \frac{1}{2}w_{,y}^2) \\ u_{,y} + v_{,x} + u_{,x}u_{,y} + v_{,x}v_{,y} + w_{,x}w_{,y} \\ u_{,z} + w_{,x} + u_{,x}u_{,z} + v_{,x}v_{,z} + w_{,x}w_{,z} \\ v_{,z} + w_{,y} + u_{zx}u_{,y} + v_z v_{,y} + w_{,z}w_{,y} \end{Bmatrix} \tag{4}$$

Where,

$$\{\varepsilon\} = \{\varepsilon\}^L + \{\varepsilon\}^{NL} \tag{5}$$

in which the strain displacement relations corresponding to the model mentioned above are

$$\{\varepsilon\}^L = \begin{Bmatrix} \varepsilon_p^l \\ 0 \end{Bmatrix} + \begin{Bmatrix} z\varepsilon_b^l \\ \varepsilon_s \end{Bmatrix} + \begin{Bmatrix} 0 \\ z^2\varepsilon_s^* \end{Bmatrix} + \begin{Bmatrix} z^3\varepsilon^* \\ 0 \end{Bmatrix},$$

$$\{\varepsilon_p^l\} = \begin{Bmatrix} u_{0,x} \\ v_{0,y} \\ u_{0,x} + v_{0,y} \end{Bmatrix}, \{\varepsilon_b^l\} = C_1 \begin{Bmatrix} \psi_{x,x} \\ \psi_{y,y} \\ \psi_{x,y} + \psi_{y,x} \end{Bmatrix},$$

$$\{\varepsilon^*\} = -C_2 \begin{Bmatrix} \psi_{x,x} \\ \psi_{y,y} \\ \psi_{x,y} + \psi_{y,x} \end{Bmatrix} - C_4 \begin{Bmatrix} \theta_{x,x} \\ \theta_{y,y} \\ \theta_{x,y} + \theta_{y,x} \end{Bmatrix}$$

$$\{\varepsilon_s\} = C \begin{Bmatrix} \psi_y \\ \psi_x \end{Bmatrix} + \begin{Bmatrix} w_{0,y} \\ w_{0,x} \end{Bmatrix}, \{\varepsilon_2^*\} = 3C_2 \begin{Bmatrix} \psi_y \\ \psi_x \end{Bmatrix} - 3C_4 \begin{Bmatrix} w_{0,y} \\ w_{0,x} \end{Bmatrix},$$

Assuming that the plate is moderately thick and strains are much smaller than the rotations, one can rewrite non-linear components of equation (4) as

$$\{\varepsilon^{NL}\} = \begin{Bmatrix} \frac{1}{2} w_{,x}^2 \\ \frac{1}{2} w_{,y}^2 \\ w_{,x} w_{,y} \\ 0 \\ 0 \end{Bmatrix} \tag{6}$$

This corresponds to the well known Von-Karman's relationships for large displacements.

The stress ± strain relations for the k_{th} lamina oriented at an arbitrary angle, y, with respect to the reference axis are

$$\begin{Bmatrix} \sigma_x \\ \sigma_y \\ \tau_{xy} \\ \tau_{xz} \\ \tau_{yz} \end{Bmatrix}_k = \begin{bmatrix} Q_{11} & Q_{12} & Q_{16} & 0 & 0 \\ Q_{21} & Q_{22} & Q_{26} & 0 & 0 \\ Q_{16} & Q_{26} & Q_{66} & 0 & 0 \\ 0 & 0 & 0 & Q_{44} & Q_{45} \\ 0 & 0 & 0 & Q_{54} & Q_{55} \end{bmatrix}_k \begin{Bmatrix} \varepsilon_x \\ \varepsilon_y \\ \gamma_{xy} \\ \gamma_{xz} \\ \gamma_{yz} \end{Bmatrix}_k \tag{7}$$

Or

$$\{\sigma_i\} = [Q_{ij}]\{\varepsilon_j\} \tag{8}$$

where $Q_{ij's}$ are the transformed stiffness coefficients.

The strain energy of the plate is given by

$$U = \frac{1}{2}\int_v \varepsilon_i^T \sigma_i dV \tag{9}$$

The five strain components (plane stress condition) may be represented as ε_i and stress components as σ_i and for linear elastic constitutive matrix C_{ij} ($C_{ij}= Q_{ij}$), the constitutive relations are given by

$$\sigma_i = C_{ij}\varepsilon_{j,} \tag{10}$$

The strain energy U can then be written as

$$U = \frac{1}{2}\iiint \{\varepsilon\}^T C_{ij}\{\varepsilon\} dxdydz$$

$$\begin{aligned} U &= \frac{1}{2}\iiint \left\{\varepsilon^L + \varepsilon^{NL}\right\}^T C_{ij}\left\{\varepsilon^L + \varepsilon^{NL}\right\}\, dxdydz \\ U &= \frac{1}{2}\iiint \left\{C_{ij}(\varepsilon^L\varepsilon^L + 2\varepsilon^L\varepsilon^{NL} + \varepsilon^{NL}\varepsilon^{NL})\right\} dxdydz \end{aligned} \tag{11}$$

The strain component ε_i can be expressed as

$$\varepsilon_i = L_i^T d + \frac{1}{2} d^t H_i d, \tag{12}$$

in which L_i is a vector, H_i is a symmetric matrix and d is the vector of displacement gradients contributing to the strains. Using the procedure adopted by Rajasekaran and Murrary for isotropic plates and Ganapathi and Varadan for composite laminates, the strain energy

expression (membrane and bending) with higher order shear deformation theory for large amplitude free vibration can be written as

$$U_{MB} = \frac{1}{2}\iint d^T [\frac{1}{2}[NA] + \frac{1}{6}[NB] + \frac{1}{12}[NC]]ddxdy \quad (13)$$

Derivative of the displacements which contribute to the strain can be expressed in vector form as

$$d^T = \{u_{,x}u_{,y}v_{,x}v_{,y}w_{,x}w_{,y}\psi_{x,x}\psi_{x,x}(\psi_{y,x}\psi_{x,y})\theta_{x,x}\theta_{y,y}(\theta_{x,x},\theta_{x,x})\}$$

The components of linear ([NA]) and non-linear stiffness matrices ([NB], [NC])

Strain energy due to shear is expressed as,

$$U_s = \frac{1}{2}\iint d_s^T [NS] d_s dxdy \quad (14)$$

Where

$$[NS] = \begin{bmatrix} [A_1] & [D_1] \\ [D_1] & [F_1] \end{bmatrix}, \quad (15)$$

And

$$(A_{ij}, D1_{ij}, F1_{ij}) = \int Q_{ij}(1, z^2, z^4)dz for i, j = 4,5.$$

The total strain energy for the laminate is therefore

$$U = U_{MB} + U_S \quad (16)$$

The kinetic energy of the laminate can be expressed in terms of nodal degrees of freedom as

$$T = \frac{1}{2}\int\left(\sum_{k=1}^{nl}\int_{z_{k-1}}^{z_k}\rho^{(k)}\bar{u}^T\bar{u}dz\right)dA \quad (17)$$

Here u is the global displacement vector and is given by

$$\{\bar{u}\} = \{u, v, w\}^T \quad (18)$$

With

$$\{\overline{u}\} = [\overline{N}\{\delta,\}] \tag{19}$$

Where

$$[\overline{N}] = \begin{bmatrix} 1 & 0 & 0 & f_1(z) & 0 & f_{21}(z) & 0 \\ 0 & 1 & 0 & 0 & f_1(z) & 0 & f_2(z) \\ 0 & 0 & 1 & 0 & 0 & 0 & 0 \end{bmatrix} \tag{20}$$

The kinetic energy T is, therefore,

$$T = \frac{1}{2}\int_A \left(\sum_{k=1}^{nl} \int_{z_{k-1}}^{z_k} \rho^{(k)} \delta^T [\overline{N}]^T [\overline{N}] \delta dz \right) dA = \frac{1}{2}\int_A \delta^T [m] \delta dA, \tag{21}$$

Where [m] is an inertia matrix, given as

$$[m] = \sum_{k=1}^{nl} \int_{z_{k-1}}^{z_k} \rho^{(k)} \varphi^T [\overline{N}]^T [\overline{N}] \varphi dz = \begin{bmatrix} p & 0 & 0 & q_1 & 0 & q_2 & 0 \\ 0 & p & 0 & 0 & q_1 & 0 & q_2 \\ 0 & 0 & p & 0 & 0 & 0 & 0 \\ q_1 & 0 & 0 & I_1 & 0 & I_3 & 0 \\ 0 & q_1 & 0 & 0 & I_1 & 0 & I_3 \\ q_2 & 0 & 0 & I_3 & 0 & I_2 & 0 \\ 0 & q_2 & 0 & 0 & I_3 & 0 & I_2 \end{bmatrix} \tag{22}$$

With $(p, q_1, q_{2,} I_1, I_2, I_3) = (\sum_{k=1}^{nl} \int_{z_{k-1}}^{z_k} \rho^k (1, f_1(z), f_2(2), f_1^2(z), f_2^2(z), [f_1(z), f_2(z)]) dz$

In the present work a C_0 nine-node isoparametric quadrilateral finite element with 7 DOF per node (u, v, w, ψ_x ,ψ_y , θ_x , θ_y) is employed. Initially the full plate is discretized using an eight element mesh; only the quarter plate is shown in Figure 2. Reduced integration is employed to evaluate the transverse shear stresses, while full integration is used for bending and stretching. Lagrangian shape functions are used to interpolate the generalized displacements within an element. The generalized displacements within the element in terms of nodal displacements can be expressed as

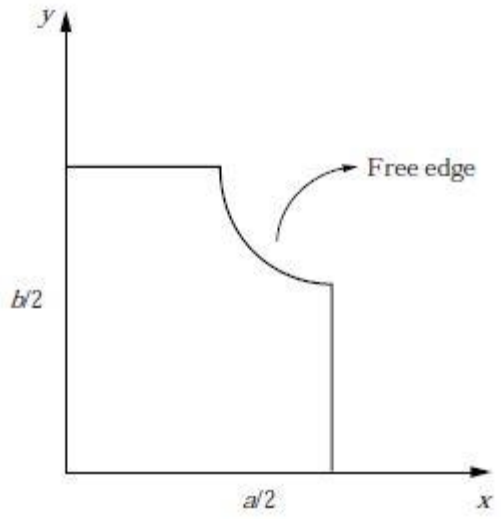

Figure3.5 Quarter plate model with co-ordinates.

$$\{\delta\}^e = \sum_{i=1}^{9} \left[N_i^e\right]\{q\}^e \tag{23}$$

The displacement gradients can be related to the nodal displacements in the finite element modelling as

$$\left[d_{bi}\right] = \begin{bmatrix} N_{i,x} & 0 & 0 & 0 & 0 & 0 & 0 \\ N_{i,y} & 0 & 0 & 0 & 0 & 0 & 0 \\ 0 & N_{i,x} & 0 & 0 & 0 & 0 & 0 \\ 0 & N_{i,y} & 0 & 0 & 0 & 0 & 0 \\ 0 & 0 & N_{i,x} & 0 & 0 & 0 & 0 \\ 0 & 0 & N_{i,y} & 0 & 0 & 0 & 0 \\ 0 & 0 & 0 & C_1 N_{i,x} & 0 & 0 & 0 \\ 0 & 0 & 0 & 0 & C_1 N_{i,y} & 0 & 0 \\ 0 & 0 & 0 & C_1 N_{i,y} & C_1 N_{i,x} & 0 & 0 \\ 0 & 0 & 0 & -C_2 N_{i,x} & 0 & -C_4 N_{i,x} & 0 \\ 0 & 0 & 0 & 0 & -C_2 N_{i,y} & 0 & -C_4 N_{i,y} \\ 0 & 0 & 0 & -C_2 N_{i,y} & -C_2 N_{i,x} & -C_4 N_{i,y} & -C_4 N_{i,x} \end{bmatrix} \{q\}, \tag{24}$$

Or

$$\left\lfloor d_{MB_i} \right\rfloor = \left[B_{MB}\right]\{q_{MB}\}, \tag{25}$$

$$[d_{si}]=\begin{bmatrix} 0 & 0 & N_{i,x} & 1 & 0 & 0 & 0 \\ 0 & 0 & N_{i,y} & 0 & 1 & 0 & 0 \\ 0 & 0 & 0 & -3 & 0 & -3 & 0 \\ 0 & 0 & 0 & 0 & -3 & 0 & 0 \end{bmatrix}\{q\} \tag{26}$$

Or

$$[d_{Si}]=[B_S]\{q_S\} \tag{27}$$

The element stiffness matrices can now be written as

$$\begin{aligned} [K_e] &= \int_{-1}^{1}\int_{-1}^{1} B_{MB}^T [NA] B_{MB} J d\psi d\eta, \\ [K_{NL1_e}] &= \int_{-1}^{1}\int_{-1}^{1} B_{MB}^T [NB] B_{MB} J d\psi d\eta, \\ [K_{NL2_e}] &= \int_{-1}^{1}\int_{-1}^{1} B_{MB}^T [NC] B_{MB} J d\psi d\eta, \\ [K_{S_e}] &= \int_{-1}^{1}\int_{-1}^{1} B_S^T [NS] B_S J d\psi d\eta, \end{aligned} \tag{28}$$

Assembling these element matrices to get global matrices and vectors, the strain energy becomes

$$U=\frac{1}{2}\iint d^T\left[\frac{1}{2}[KMB]+\frac{1}{6}[K_{NL1}]+\frac{1}{12}[K_{NL2}]+\frac{1}{2}[K_S]\right]ddxdy \tag{29}$$

The Lagrangian equation of motion for free vibration is given by

$$\frac{d}{dt}\left(\frac{\partial T}{\partial q_i}\right)-\frac{\partial U}{\partial q_i}=0 \tag{30}$$

Substituting the strain energy and kinetic energy expressions into equation (30), the governing equation for the non-linear eigenvalue problem is obtained as

$$[M]\left\{\ddot{\delta}\right\}+\left[[K_{MB}]+\frac{1}{2}[K_{NL1}]+\frac{1}{3}[K_{NL2}]+[K_S]\right]\{\delta\}=0 \tag{31}$$

Equation (31) is solved using the solution procedure for the direct iteration method .

At the point of maximum amplitude

$$\left\{\ddot{\delta}\right\} = -\omega^2 \{\delta\}, \left\{\dot{\delta}\right\} = 0.$$

Let

$$\left[K^L\right] = \left[K_{MB}\right] + \left[K_S\right] \tag{32}$$

$$\left[K^{NL}\right] = \frac{1}{2}\left[K_{NL1}\right] + \frac{1}{3}\left[K_{NL2}\right] \tag{33}$$

The non-linear eigenvalue problem is now reduced to

$$\left[K^L + K^{NL}(\delta)\right]\{\delta\} - \omega^2 [M]\{\delta\} = 0 \tag{34}$$

CHAPTER 4

RESULTS AND DISCUSSIONS

4.1 OVERVIEW

In this chapter we are going to discuss the vibration and stability of a structure subjected to geometrical discontinuities like cutout, delamination by using numerical method. The present study compares the results with previously done work in the literature to validate the model and then the parametric study carried out by varying the parameters like number of layers, Aspect Ratio, percentage of geometrical discontinuities and Boundary conditions.

4.2 COMPOSITE PLATE WITH DELAMINATION

4.2.1 CONVERGENCE STUDY

The convergence study is done for free vibration of a delaminated composite panel. The delaminated square plate is subjected to simply supported boundary condition with varying mesh sizes and fiber orientation. The result shows that the value converges well with the 8 X 8 mesh.

Table 4.1: Convergence Study for Composite Panel

Mesh size	**Free vibration (Natural frequency in Hz)**					
Ply Orientation	**$(0/0)_2$**		**$(0/90)_2$**		**$(45/-45)_2$**	
% of Delamination	**0**	**25**	**0**	**25**	**0**	**25**
4*4	100.6057	67.4311	92.9095	54.5393	124.4539	92.7280
8*8	100.4132	66.0083	92.7162	52.9373	124.2571	90.8396
12*12	100.4076	65.9525	92.7110	52.8493	124.2504	90.7042

4.2.2 VALIDATION OF THE MODEL

The result on free vibration of delaminated simply supported plate are compared with result by Parhi et al. (2001) , Namita et al. (2012) having the material properties given below. The program of the finite element formulation is developed in MATLAB and validated by comparing the present study with those available in the existing literature. For this free vibration analysis, the simply supported boundary conditions is used. Table 4.2 shows the validation of results for delaminated composite plate subjected to simply supported boundary conditions with the literature.

The following are geometric and material properties.

$a = b = 0.5m$, $a/h=100$, $\mu 12=0.25$, $\rho=1600kg/m_3$, $E11=172.5Gpa$

$E_{22}=6.9Gpa$, $G_{12}=G_{13}=3.45Gpa$, $G_{23}=1.38Gpa$

Table 4.2: Validation Study for Composite Plate

Ply orientation	**% of Delamination**	**Parhi et al. (2001)**	**Namita et al. (2012)**	**Present Work**
$(0/90)_2$	0	92.87	92.72	92.71
$(45/-45)_2$	0	124.26	124.26	124.25
$(0/90)_2$	25	52.93	52.94	52.93
$(45/-45)_2$	25	90.86	90.84	90.83

4.2.3 PARAMETRIC STUDY ON COMPOSITE PLATE

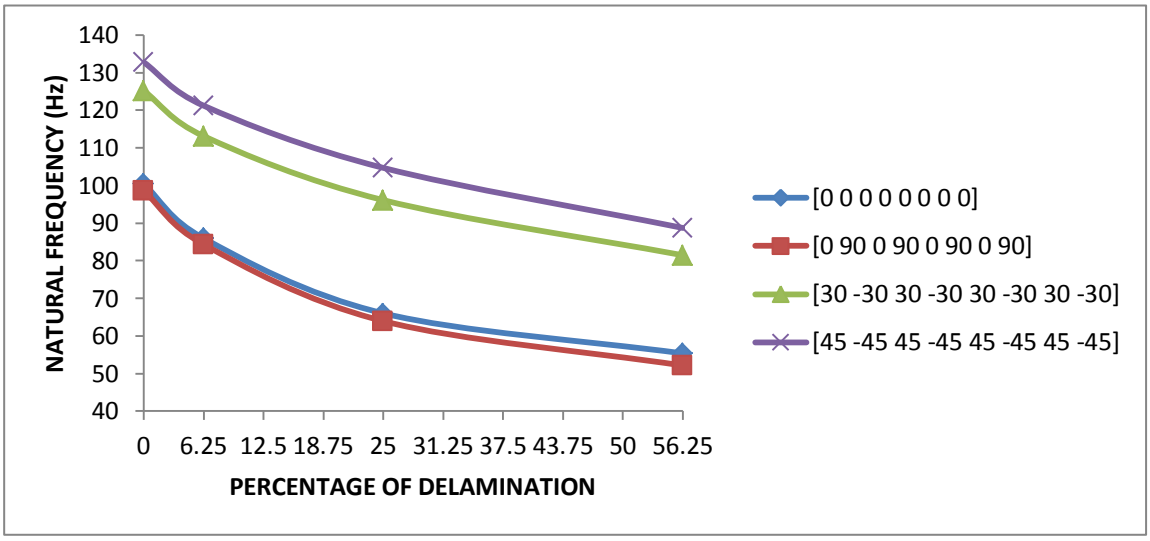

Figure 4.1: Effect of % of delamination on Natural frequency for SSSS boundary conditions and aspect ratio of 1 for various ply orientation

The figure 4.1 clearly shows that the natural frequencies of angle ply composites are more than the cross ply composites. The values of natural frequency of $[45\ -45\ 45\ -45]_2$ for 6.25%, 25%, 56, 25% increases at a rate of 6% to 8%, 30% to 40%, and 29% to 37% respectively when compared with $[30\ -30\ 30\ -30]_2$, $[0\ 90\ 0\ 90]_2$ and $[0\ 0\ 0\ 0]_2$ ply orientation.

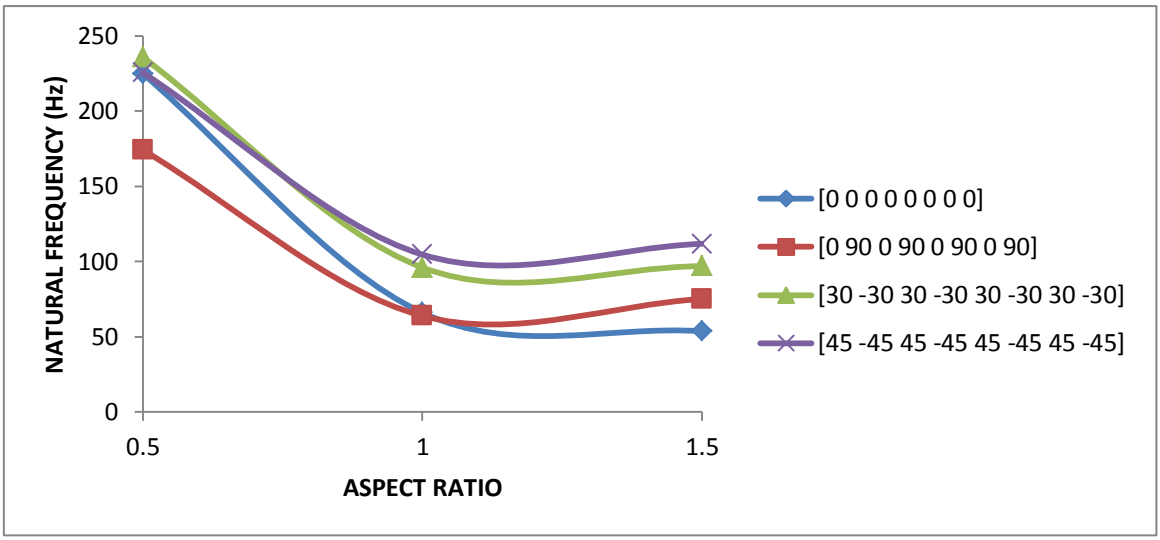

Figure 4.2: Effect of aspect ratio on natural frequency for SSSS boundary conditions with 25% delamination

The figure 4.2 shows that the aspect ratio of 0.5 has the highest natural frequency compared to other aspect ratios of 1 and 1.5. As the aspect ratio increases from 0.5 to 1.5 the natural frequency of the composite plate decreases by about 50%, 59%, 56% for the ply orientation of $[45\ -45]_{4,}$ $[30\ -30]_4$, $[0\ 90]_4$ respectively.

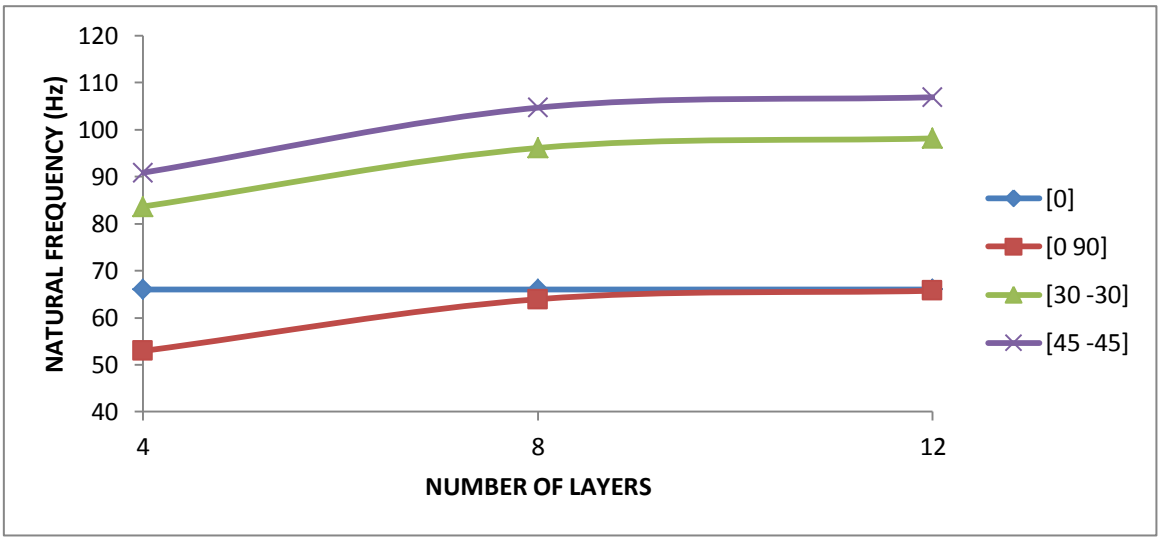

Figure 4.3: Effect of number of layers on natural frequency for SSSS boundary conditions with 25% delamination

The figure 4.3 shows that as the numbers of layers are increased, the natural frequency increases. As the number of layers increases from 4 to 12 the natural frequencies of the composite plate increases by 15%, 15%, 20% for the ply orientation of $[45\ -45]_4$, $[30\ -30]_4$, $[0\ 90]_4$ respectively. It has been observed that the natural frequency remains constant for the ply orientation of $[0\ 0]_4$ even if the number of layers are increased.

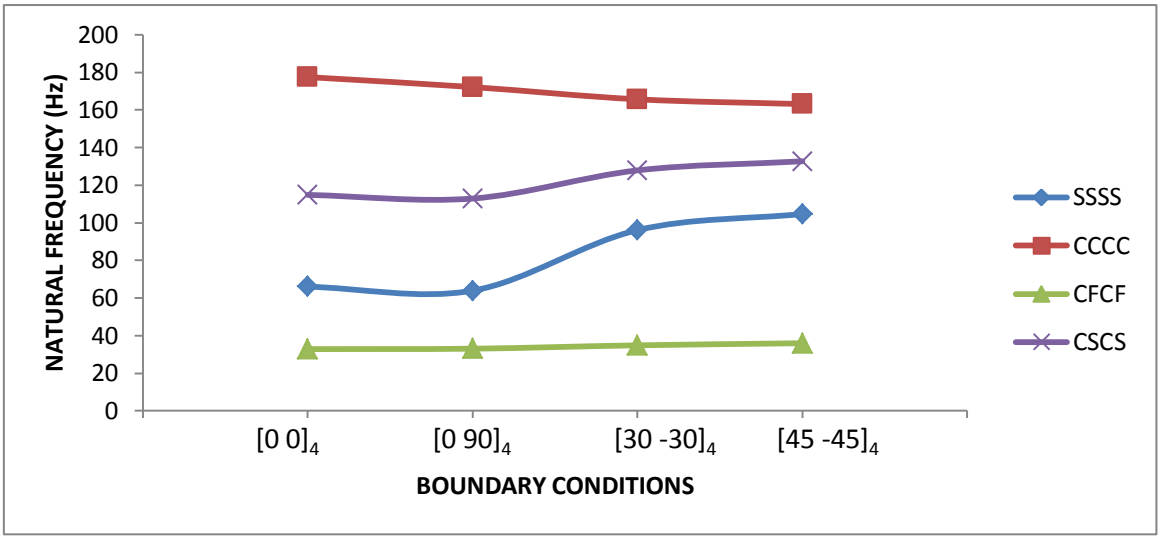

Figure 4.4: Effect of boundary condition on natural frequency for 25% delamination with aspect ratio 1

The figure 4.4 shows that the effect of boundary condition on natural frequency of the composite plates for different ply orientation. It can be seen that the CCCC boundary condition has the highest natural frequency for different ply orientation.

4.3 COMPOSITE CYLINDRICAL SHELL WITH DELAMINATION

4.3.1 VALIDATION OF THE MODEL

The result on free vibration of delaminated simply supported cylindrical shell are compared with result by Parhi et al. (2001) and Namita et al. (2012) having the material properties given below. The program of the finite element formulation is developed in MATLAB and validated by comparing the present study with those available in the existing literature. For this free vibration analysis, the simply supported boundary conditions is used. Table 4.3 shows the validation of results for delaminated composite cylindrical shell subjected to simply supported boundary conditions with the literature.

The following are geometric and material properties.

$a = b = 0.5m$,$a/h=100$,$\mu_{12}=0.25$, $\rho=1600kg/m_3$,$E_{11}=172.5Gpa$

$E_{22}=6.9Gpa$, $G_{12}=G_{13}=3.45Gpa$, $G_{23}=1.38Gpa$

$Ry/a=10$ [Rx= infinity]

Table 4.3: Natural frequencies (Hz) for mid-plane delaminated cylindrical shell subjects to simply supported boundary conditions.

Ply orientation	% of Delamination	Parhi et al. (2001)	Namita et al. (2012)	Present Work
$(0/90)_2$	0	103.03	103.02	103.05
$(45/-45)_2$	0	193.38	193.37	193.38
$(0/90)_2$	25	69.60	69.59	69.60
$(45/-45)_2$	25	168.02	168.04	168.05

4.3.2 PARAMETRIC STUDY ON CYLINDRICAL SHELL

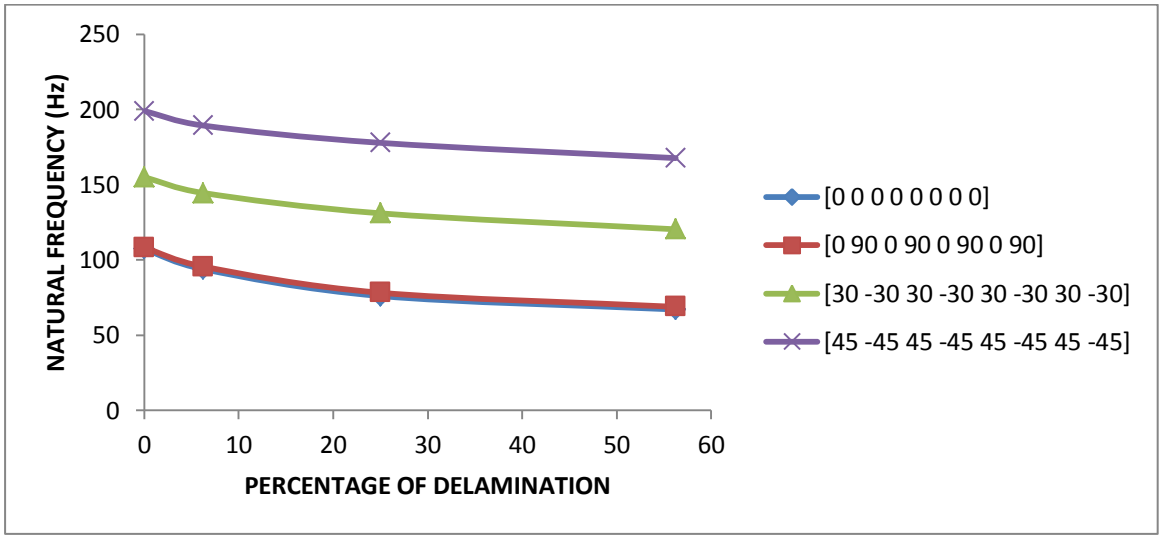

Figure 4.5: Effect of % of delamination on Natural frequency for SSSS boundary conditions and aspect ratio of 1 for various ply orientation.

The figure 4.5 shows that the natural frequency of angle ply composites is more than the cross ply composites. As the percentage of delamination increases from 6.25% to 25% the natural frequencies of the composite cylindrical shell decreases by about 11% , 16% ,28% for $[45\ -45]_4$,$[30\ -30]_4$,$[0\ 90]_4$ ply orientations respectively.

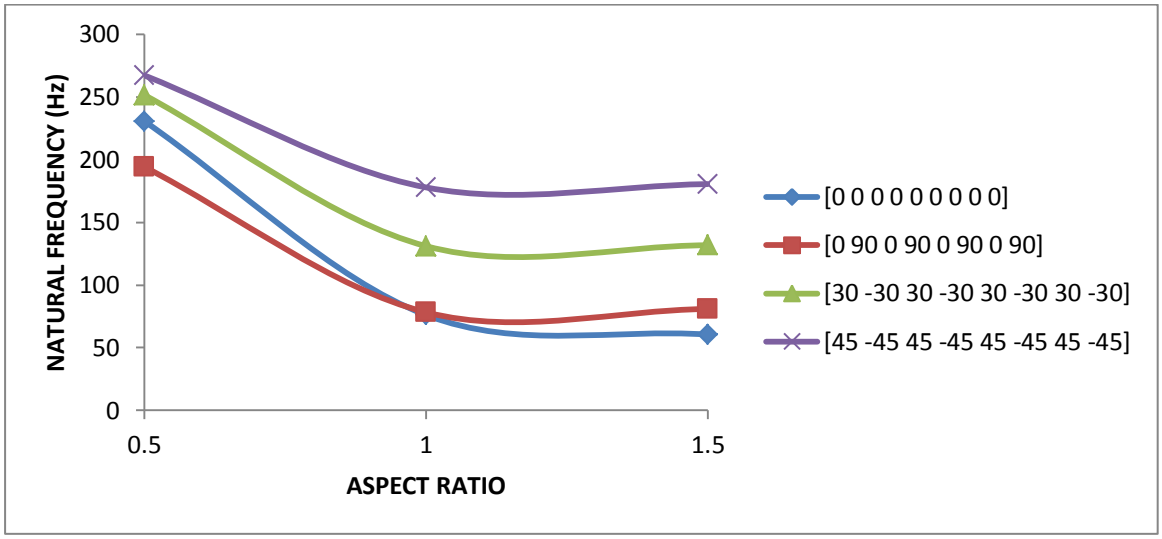

Figure 4.6: Effect of aspect ratio on Natural frequency for SSSS boundary condition with 25% delamination.

The figure 4.6 shows that the aspect ratio of 0.5 has the highest natural frequency and there is a slight variation in the natural frequencies when compared to the aspect ratios of 1 and 1.5. As the aspect ratio increases from 0.5 to 1.5, the natural frequency of the composite plate decreases by about 32%, 47%, 58% for the ply orientation of $[45\ -45]_4$, $[30\ -30]_4$, $[0\ 90]_4$ respectively.

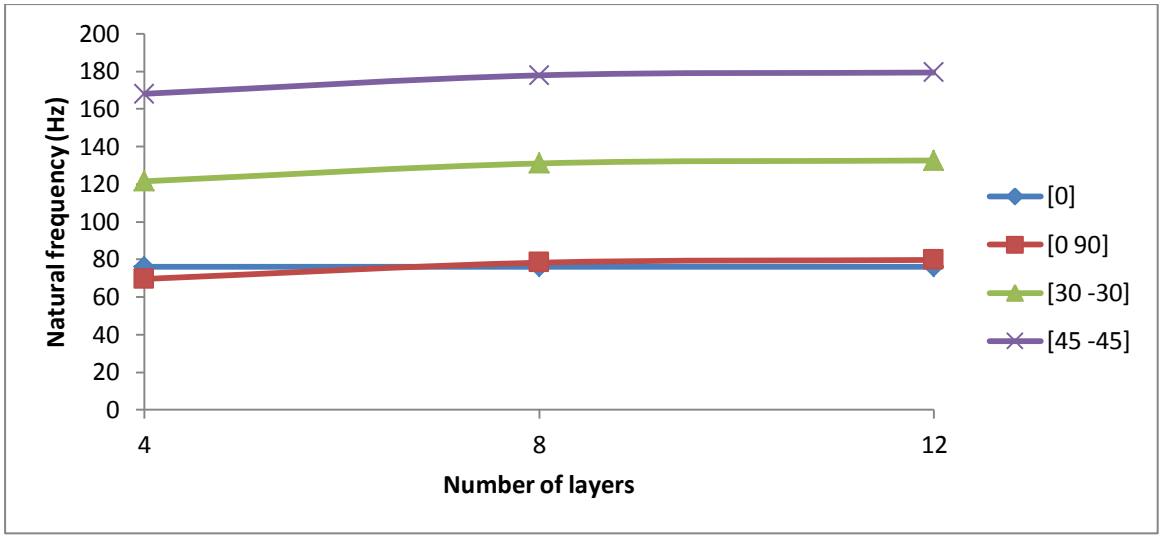

Figure 4.7: Effect of number of layers on Natural frequency for SSSS boundary condition with 25% delamination

The figure 4.7 shows that as the number of layers increases, the natural frequency increases. As the number of layers increases from 4 to 12 the natural frequencies of the composite plate increases by 6%,8%,12% for the ply orientation of $[45\ -45]_4$, $[30\ -30]_4$, $[0\ 90]_4$ respectively. It has been observed that the natural frequency remains constant for the ply orientation of $[0\ 0]_4$ even if the number of layers are increased.

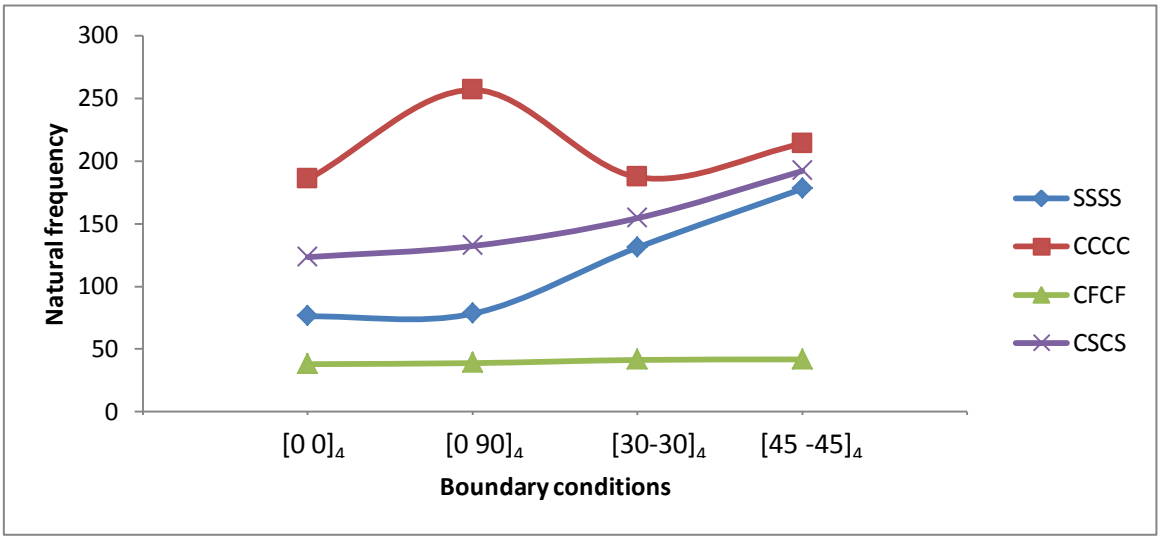

Figure 4.8: Effect of boundary condition on natural frequency for 25% delamination and aspect ratio 1.

The figure 4.8 shows that, the effect of boundary condition on natural frequency of the cylindrical shells for different ply orientation. It can be seen that the CCCC boundary condition has the highest natural frequency for different ply orientation.

4.4 COMPOSITE SPHERICAL SHELL WITH DELAMINATION

4.4.1 VALIDATION OF THE MODEL

The result on free vibration of delaminated simply supported spherical shell are compared with result by Parhi et al. (2001) and Namita et al. (2012) having the material properties given below. The program of the finite element formulation is developed in MATLAB and validated by comparing the present study with those available in the existing literature. For this free vibration analysis, the simply supported boundary conditions is used. Table 4.4 shows that the validation of results for delaminated composite cylindrical shell subjected to simply supported boundary conditions with the literature.

The following are geometric and material properties.

$$a = b = 0.5\ m,\ a/h=100,\ \mu_{12}=0.25,\ \rho=1600kg/m_3,\ E_{11}=172.5Gpa$$

$$E_{22}=6.9Gpa,\ G_{12}=G_{13}=3.45Gpa,\ G_{23}=1.38Gpa$$

$$R_x=R_y=5$$

Table 4.4: Natural frequencies (Hz) for mid-plane delaminated spherical shell subjected to simply supported boundary conditions.

Ply orientation	% of Delamination	Parhi et al. (2001)	Namita et al. (2012)	Present Work
$(0/90)_2$	0	129.20	129.14	129.19
$(45/-45)_2$	0	301.13	301.13	301.13
$(0/90)_2$	25	104.59	104.56	104.58
$(45/-45)_2$	25	225.10	225.13	225.19

4.4.2 PARAMETRIC STUDY ON SPHERICAL SHELL

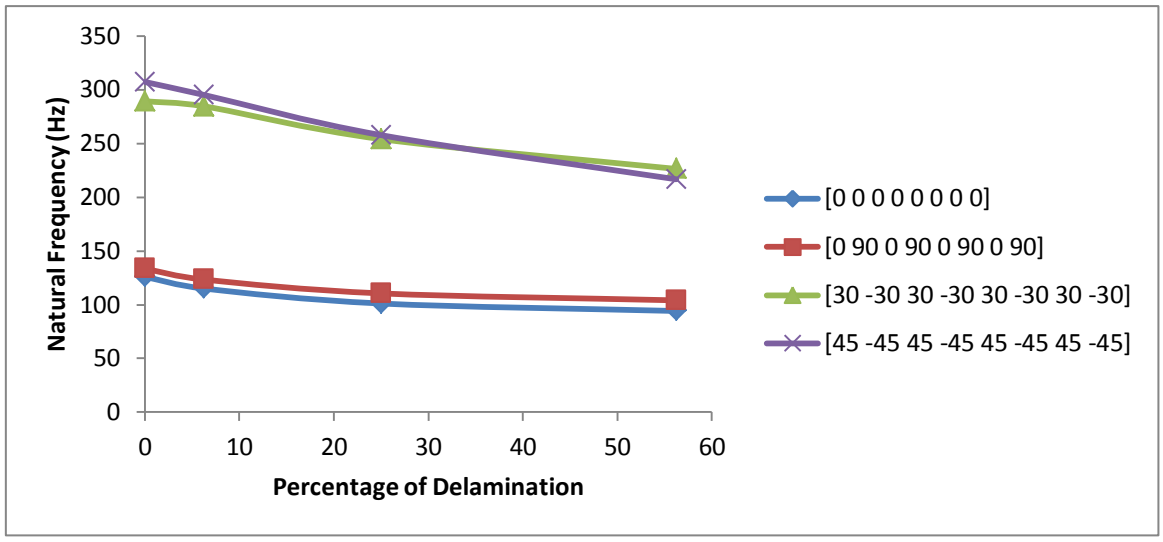

Figure 4.9: Effect of % delamination on natural frequency for SSSS boundary condition with aspect ratio 1

The figure 4.9 shows that the natural frequency of angle plies composite panels are more than the cross ply composites panels. As the percentage of delamination increases from 6.25% to 25% the natural frequencies of the composite cylindrical shell decreases by about 26% , 20% ,15% for $[45\ -45]_4$,$[30\ -30]_4$,$[0\ 90]_4$ ply orientations respectively.

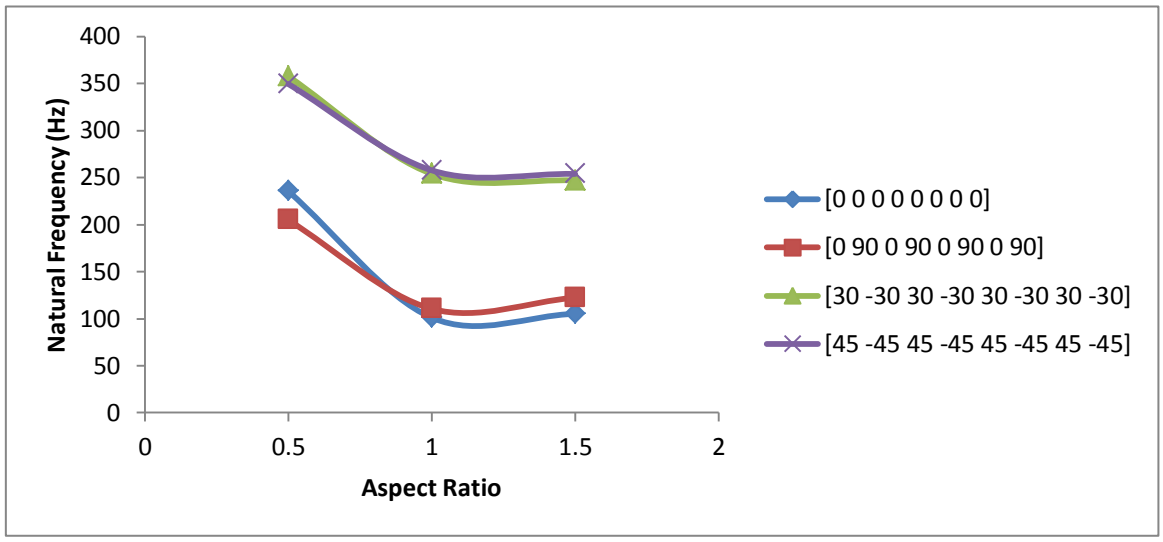

Figure 4.10: Effect of aspect ratio on natural frequency for SSSS boundary condition with 25% delamination

The figure 4.10 shows that the aspect ratio of 0.5 has the highest natural frequency and there is a slight variation in the natural frequencies when compared to the aspect ratios 1 and 1.5. As the aspect ratio increases from 0.5 to 1.5 the natural frequency of the composite plate decreases by about 27%, 31%, 40% for the ply orientation of $[45\ -45]_4$, $[30\ -30]_4$, $[0\ 90]_4$ respectively.

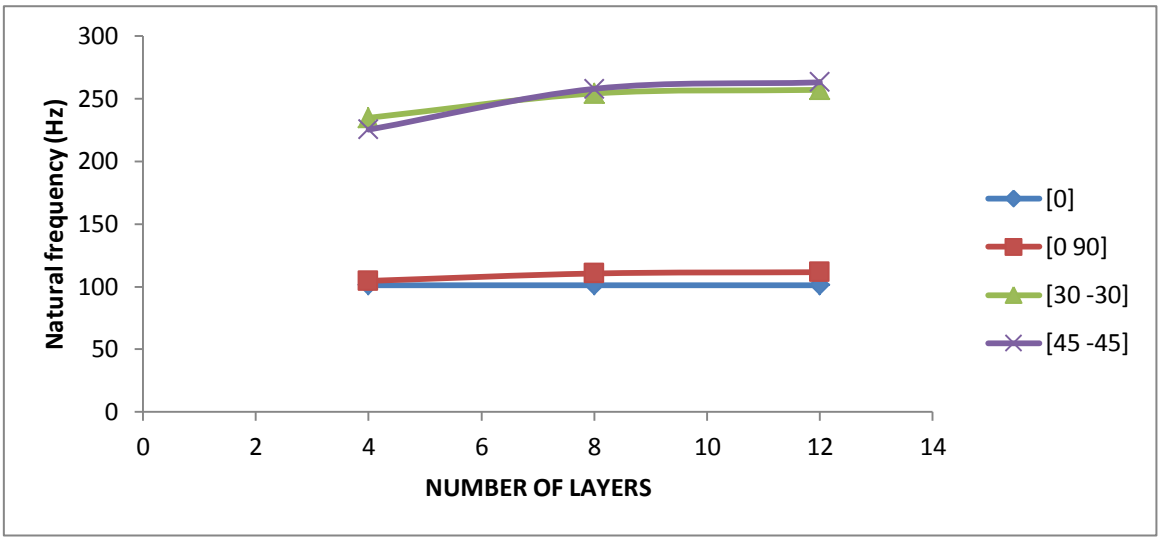

Figure 4.11: Effect of number of layers on natural frequency for SSSS boundary condition with 25% delamination.

The figure 4.11 shows that as the number of layers are increased the natural frequency increases. As the number of layers increases from 4 to 12 the natural frequencies of the composite plate increases by 14%, 8%, 6% for the ply orientation of $[45\ -45]_4$, $[30\ -30]_4$, $[0\ 90]_4$ respectively. It has been observed that the natural frequency of the ply orientation remains constant even if the numbers of layers are increased.

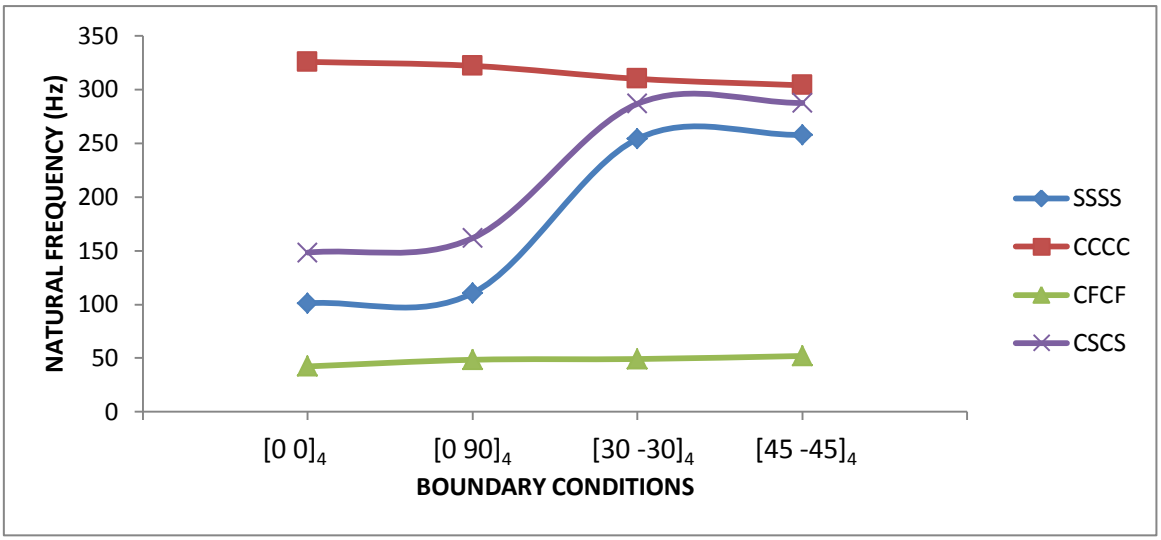

Figure 4.12: Effect of boundary condition on natural frequency for 25% delamination and aspect ratio 1.

The figure 4.12 shows that, the effect of boundary condition on natural frequency of the spherical shells for different ply orientation. It can be seen that the CCCC boundary condition has the highest natural frequency for different ply orientation.

4.5 EFFECT OF CURVATURE ON NATURAL FREQUENCIES OF COMPOSITE PANELS

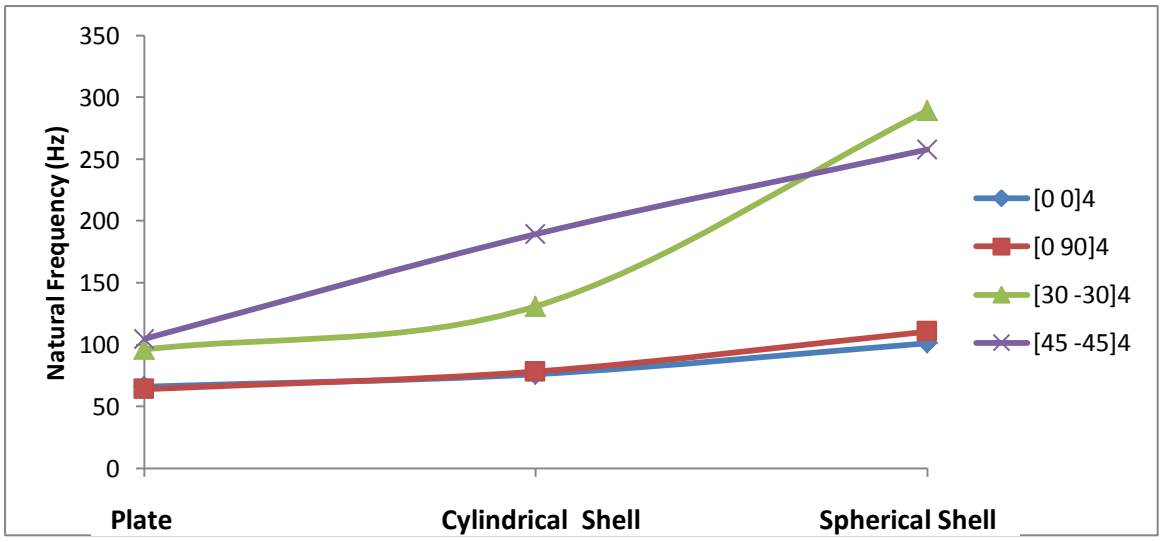

Figure 4.13: Effect of curvature on natural frequency for 25% Cutout and aspect ratio 1.

The figure 4.13 shows the effect of curvatures on natural frequency of delaminated composite panels. It can be seen that as the curvature reduces the natural frequency of the composite panel increases.

4.6 COMPOSITE PLATE WITH CUTOUT

4.6.1 VALIDATION OF THE MODEL

The result on free vibration of a plate having cutout subjected to CSCF boundary condition are compared with result by Chai (1996), having the material properties given below. The problem has been solved using a finite element method by using ABAQUS CAE software and validated by comparing the present study with those available in the existing literature. Table 4.5 shows the validation of results for a composite plate subjected to CSCF boundary conditions with Cutout in the literature.

The following are geometric and material properties.

$a = 0.448m$, $b= 0.121m$, $\mu 12=0.28$, $\rho=1600kg/m_3$, $E_{11}=130Gpa$

$E_{22}=9Gpa$, $G_{12}=G_{13}=4.8Gpa$, $G_{23}=4.8Gpa$

Table 4.5: Validation of Model with Natural Frequency (Hz)

Specimen 1 d=0		**Specimen 2 d=22mm**		**Specimen 3 d=35mm**		**Specimen 4 d=44mm**		**Specimen 5 d=57mm**	
Chai (1996)	**Present Work**	**Chai (1996)**	**Present Work**	**Chai (1996)**	**Present Work**	**Chai (1996)**	**Present Work**	**Chai (1996)**	**Present Work**
80	79.504	80	79.611	80	79.778	80	80.161	81	80.953

The result on buckling load of a plate having cutout subjected to SSSS boundary condition are compared with result by Anil et al (2007), having the material properties given below. The problem has been solved using a finite element method by using ABAQUS CAE software and validated by comparing the present study with those available in the existing literature. Table 4.6 shows the validation of results for a composite plate subjected to SSSS boundary conditions with Cutout in the literature.

The following are geometric and material properties.

$a/b=1$, $\mu_{12}=0.25$, $\rho=1600kg/m_3$, $E_{11}=200Gpa$

$E_{11}/E_{22}=49$, $G_{12}/E_{22}=G_{13}/E_{22}=0.6$, $G_{23}/E_{22}=0.5$

Table 4.6: Validation of Model with Non dimensional Buckling loads $\left[\frac{N_y b^2}{E_t h^3}\right]$

Thickness ratio(a/h)	Reddy et al	Anil et al	Present
10	25.828	25.943	25.954
5	12.224	12.603	12.422

4.6.2 VIBRATION STUDY

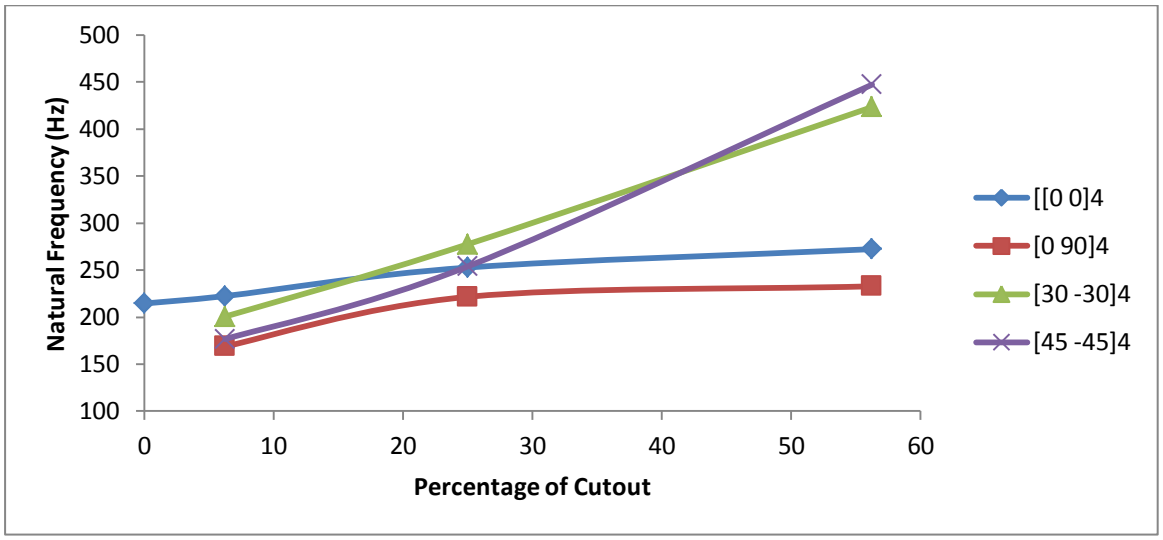

Figure 4.14: Effect of % of Cutout on Natural frequency for SSSS boundary conditions and aspect ratio of 1 for various ply orientation

The figure 4.14 shows that the natural frequencies of angle ply composites are more than the cross ply composites. It should be noted that as the percentage of cutout increases from 6.25% to 25% the natural frequencies of the composite plate increases by about 23% , 27%, 30% for $[45\ -45]_4$,$[30\ -30]_4$,$[0\ 90]_4$ ply orientations respectively.

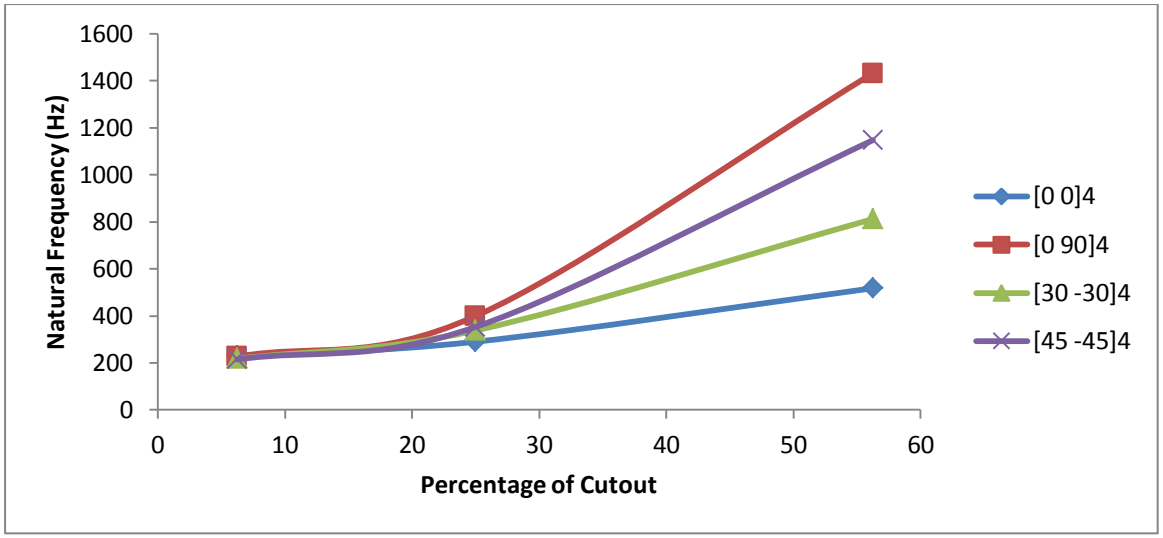

Figure 4.15 Effect of % of Cutout on Natural frequency for CCCC boundary conditions and aspect ratio of 1 for various ply orientation.

The figure 4.15 shows that the natural frequencies of angle ply composites are more than the cross ply composites. It should be noted that the frequency for 6.25% cutout area is almost same for all ply orientations and as the percentage of cutout increases from 6.25% to 25% the natural frequencies of the composite plate increases by about 38% , 35%, 43% for $[45\ -45]_4$,$[30\ -30]_4$,$[0\ 90]_4$ ply orientations respectively.

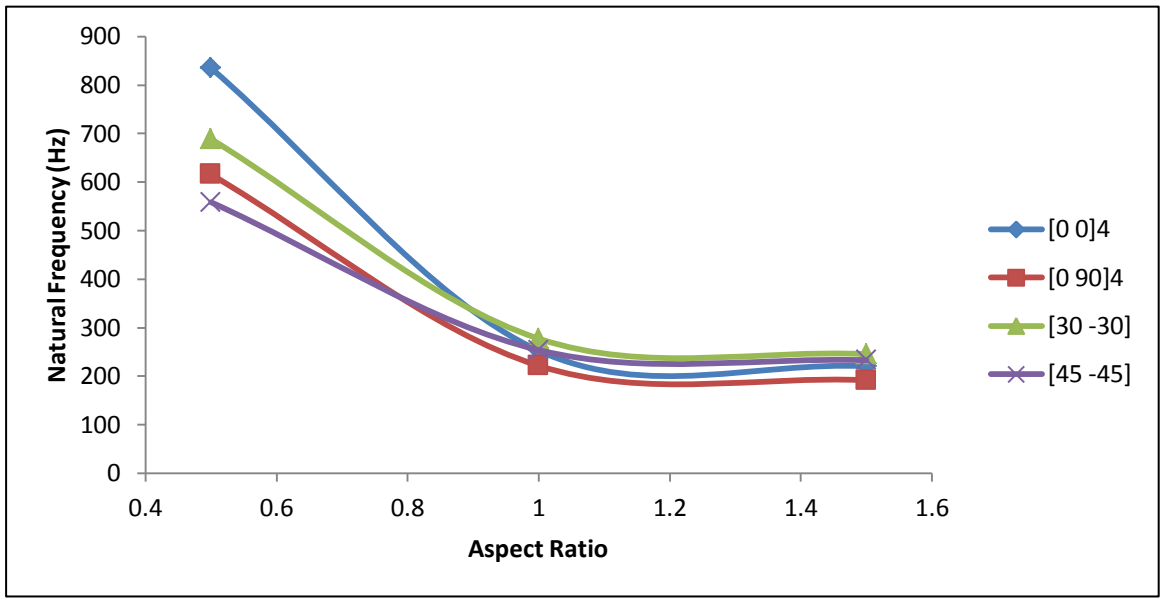

.**Figure 4.16:** Effect of aspect ratio on natural frequency for SSSS boundary condition with 25% Cutout.

The figure 4.16 shows that the aspect ratio of 0.5 has the highest natural frequency and there is a slight variation in the natural frequencies when compared to the aspect ratios 1 and 1.5. As the aspect ratio increases from 0.5 to 1.5 the natural frequency of the composite plate decreases by about 58%, 64%, 69% for the ply orientation of $[45\ -45]_4$, $[30\ -30]_4$, $[0\ 90]_4$ respectively.

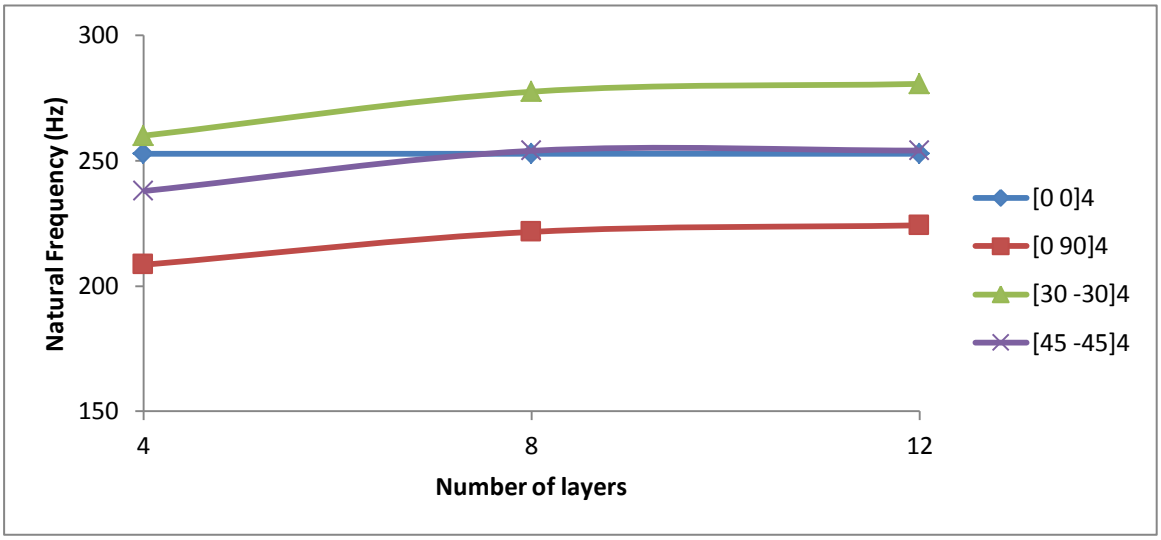

Figure 4.17: Effect of number of layers on Natural frequency for SSSS boundary condition with 25% Cutout.

The figure 4.17 shows that as the number of layers are increased the natural frequency increases. As the number of layers increases from 4 to 12 the natural frequencies of the composite plate increases by 6%,7%,7% for the ply orientation of $[45\ -45]_4$, $[30\ -30]_4$, $[0\ 90]_4$ respectively. It has been observed that the natural frequency remains constant for the ply orientation of $[0\ 0]_4$ even if the number of layers are increased.

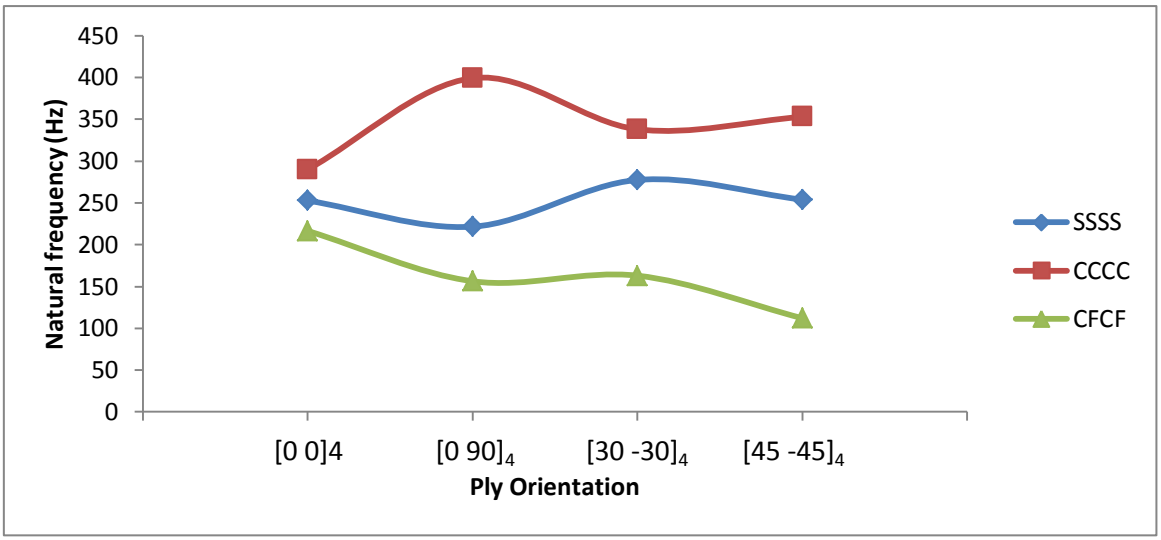

Figure 4.18: Effect of boundary condition on natural frequency for 25% Cutout and aspect ratio 1.

The figure 4.18 shows that, the effect of boundary condition on natural frequency of the composite plate with cutout for different ply orientation. It can be seen that the CCCC boundary condition has the highest natural frequency for different ply orientation.

4.6.3 STABILITY STUDY

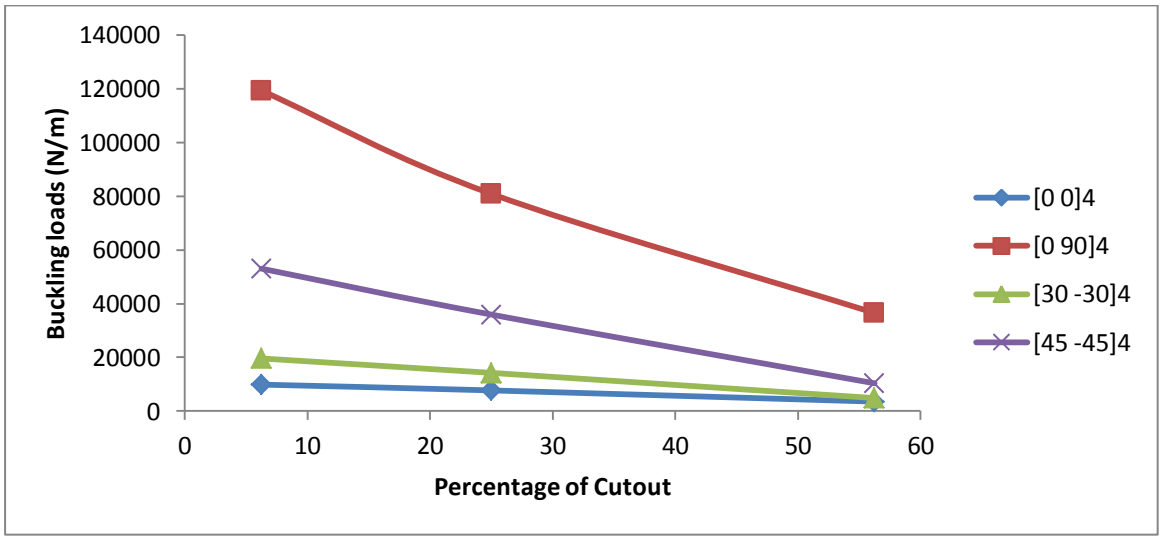

Figure 4.19: Effect of % of Cutout on buckling load for CFCF boundary conditions and aspect ratio of 1 for various ply orientation.

The figure 4.19 shows that the natural frequencies of cross ply $[0\ 90]_4$ composites are more than the angle ply composites. It should be noted that as the percentage of cutout increases

from 6.25% to 25% the buckling load of the composite plate decreases by about 80% , 75%, 69% for [45 -45]4 ,[30 -30]4 ,[0 90]4 ply orientations respectively.

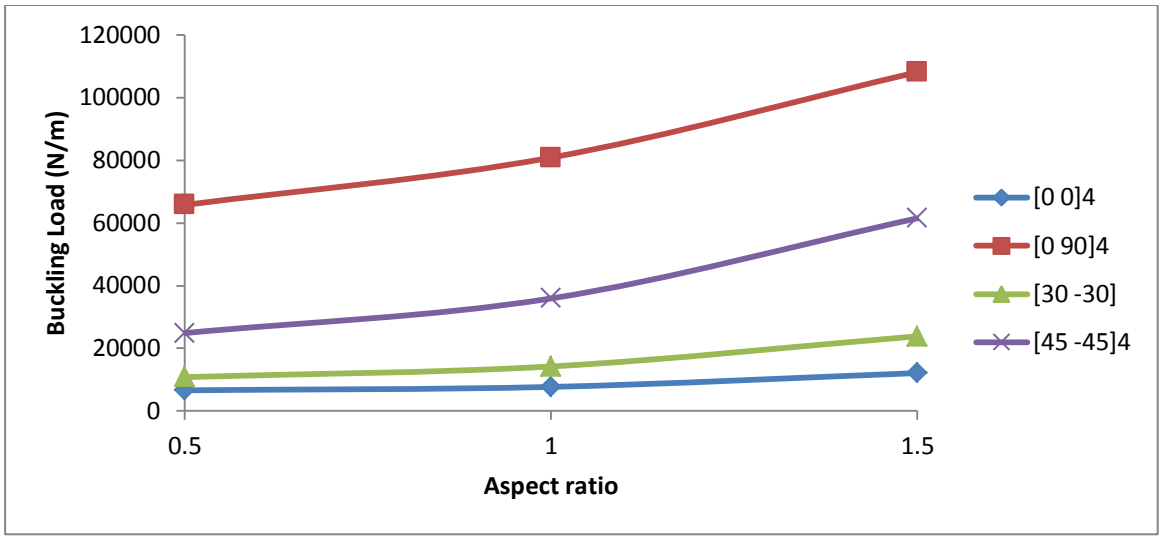

Figure 4.20: Effect of aspect ratio on buckling load for CFCF boundary conditions and percentage cutout of 25% for various ply orientation.

The figure 4.20 shows that the aspect ratio of 1.5 has the highest natural frequency. As the aspect ratio increases from 0.5 to 1.5 the natural frequency of the composite plate increases by about 59%, 54%, 39% for the ply orientation of $[45\ -45]_4$, $[30\ -30]_4$, $[0\ 90]_4$ respectively.

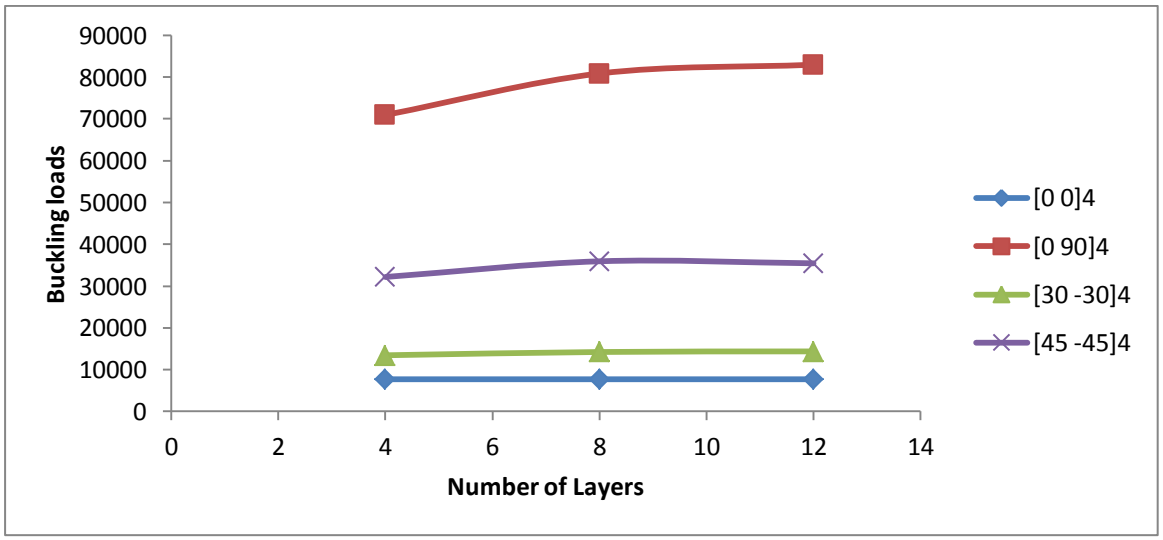

Figure 4.21: Effect of number of layers on buckling load for CFCF boundary conditions and percentage cutout of 25% for various ply orientation.

The figure 4.21 shows that the buckling loads of cross ply $[0\ 90]_4$ composites are more than the angle ply composites. It should be noted that as the number of layers increases from 4 to 12 the buckling load of the composite plate increases by about 9% , 6%, 14% for [45 -45]4 ,[30 -30]4 ,[0 90]4 ply orientations respectively.

CHAPTER 5

CONCLUSIONS AND FUTURE SCOPE

5.1 CONCLUSION

Based on first order shear deformation theory, the vibration and stability analysis of composite panels subjected to geometrical discontinuities is carried out and followings are the salient conclusions obtained from the present study ,

1. The delamination of composite laminates plays an important role in degrading the natural frequencies of the laminates. The natural frequencies of composite panels decrease with increase in delamination due to reduction of stiffness for all laminates.
2. The natural frequencies of free vibration of composite plates subjected to cutouts may increase or decrease depending on where the cutout is placed.
3. The effects of delamination and cutout on natural frequencies are greatly dependent on the boundary conditions, that is, the more strongly the plate is restrained, the greater the effects on the natural frequencies.
4. The frequencies of vibration are the lowest in C-F-C-F boundary condition and the highest in C-C-C-C cases for all laminates as observed here with several boundary conditions.
5. The composite plate with C-F-C-F boundary condition is the worst affected among all boundary conditions with delamination area 25% or more with reference to frequency of vibration.
6. The effect of having more number of layers in the composite plate results in the increase in natural frequency.

7. The natural frequencies are the lowest for 1.5 aspect ratio and the highest in 0.5 aspect ratio for all laminates as observed here with SSSS boundary condition.
8. The natural frequencies are largely influenced by the curvature. The natural frequency of a spherical shell is more than the natural frequency of cylindrical shell and plate.
9. The buckling load of the composite plates gets reduced as the area of cutout increases.
10. The buckling load of composite plates gets increased as the aspect ratio is increased.
11. The buckling load of the composite plate increases with the increase in number of layers.

5.2 FUTURE SCOPE OF STUDY

In the present study the natural frequency and buckling load of the laminated plate was determined. The effect of area of delamination and cutout, aspect ratio, fiber orientation and number of layers on natural frequency and buckling load was studied. The future scope of the present investigation can be expressed as follows,

(a) Buckling analysis of delaminated industry driven woven composite plates with and without cutouts.

(b) Buckling analysis of laminated woven fiber composite plates with delamination by numerical approach for different boundary conditions.

(c). Dynamic stability of woven fiber laminated and delaminated composite plates with and without cutout.

REFERENCES

1. A.L. Poore, A. Barut, E. Madenci, Free vibration of laminated cylindrical shells with a circular cutout, Journal of Sound and Vibration 312 (2008) 55–73.
2. Dinesh Kumar, S.B. Singh, Stability and failure of composite laminates with various shaped cutouts under combined in-plane loads, Composites : Part B 43 (2012) 142-149.
3. F. Ju, H. P. Lee and K. H. Lee, Finite Element Analysis Of Free Vibration Of Delaminated Composite Plates, Composites Engineering, Vol. 5, No. 2, pp. 195-209, 1995
4. F.Ju, H. P. Lee & K. H. Lee, Free vibration of composite plates with delaminations around cutouts, Composite Structures 31 (1995) 177-183.
5. Giulio Romeo, Analytical and Experimental Behaviour of Laminated Panels with Rectangular Opening under Biaxial Tension, Compression and Shear Loads, Journal of Composite Materials 2001 35: 639, DOI: 10.1177/002199801772662037.
6. H. P. Lee, S. P. Lim and S. T. Chow, Free Vibration of Composite Rectangular Plates with Rectangular Cutouts, Composite Structures 8 (1987) 63-81
7. Hamit Akbulut and Tolga Ura, An Investigation on Buckling of Composite Laminated Plates with Corner Circular Notches, Journal of Thermoplastic Composite Materials 2007 20: 371, DOI: 10.1177/0892705707079608.
8. Haoran Chen, Ming Hong, Yuandong Liu, Dynamic behavior of delaminated plates considering progressive failure process, Composite Structures 66 (2004) 459–466.
9. J.P. Hou, G. Jeronimidis, Vibration of delaminated thin composite plates, Composites: Part A 30 (1999) 989–995.
10. Jinho Oh a, Maenghyo Cho a, Jun-Sik Kim, Dynamic analysis of composite plate with multiple delaminations based on higher-order zigzag theory, International Journal of Solids and Structures 42 (2005) 6122–6140
11. K. Sivakumar, N. G. R. Iyengar, Free Vibration Of Laminated Composite Plates With Cutout, Journal of Sound and Vibration (1999) 221(3), 443-470
12. K.S. Sai Ram, T. Sreedhar Babu, Free vibration of composite spherical shell cap with and without a cutout, Computers and Structures 80 (2002) 1749–1756

13. L.H. Yam, Z. Wei, L. Cheng, W.O. Wong, Numerical analysis of multi-layer composite plates with internal delamination, Computers and Structures 82 (2004) 627–637.
14. Lazarus H. Tenek, Edmund G. Henneke II & Max D. Gunzburger , Vibration of delaminated composite plates and some applications to non-destructive testing, Composite Structures 23 (1993) 253-262
15. M. Aydin Komur, Faruk Sen, Akın Atas, Nurettin Arslan, Buckling analysis of laminated composite plates with an elliptical/circular cutout using FEM, Advances in Engineering Software 41 (2010) 161–164.
16. M. K. Pandit, S. Haldar And M. Mukhopadhyay, Free Vibration Analysis of Laminated Composite Rectangular Plate Using Finite Element Method, Journal of Reinforced Plastics and Composites 2007 26: 69, DOI: 10.1177/0731684407069955.
17. Murat Yazici, Resat Ozcan And Sedat Ulku, Buckling of Composite Plates With U-shaped Cutouts, Journal of Composite Materials 2003 37: 2179, DOI: 10.1177/002199803038109.
18. N. Hua; H. Fukunaga, M. Kameyama, Y. Aramaki, F.K. Chang, Vibration analysis of delaminated composite beams and plates using a higher-order finite element, International Journal of Mechanical Sciences 44 (2002) 1479–1503
19. Namita Nanda and J.N. Bandyopadhyay, Nonlinear Free Vibration Analysis of Laminated Composite Cylindrical Shells with cutouts, Journal of Reinforced Plastics and Composites 2007 26: 1413 originally published online 26 July 2007 , DOI: 10.1177/0731684407079776
20. P. K. Parhi, S. K. Bhattacharyya and P. K. Sinha, Finite Element Dynamic Analysis of Laminated Composite Plates with Multiple Delaminations, Journal of Reinforced Plastics and Composites 2000 19: 863, DOI: 10.1177/073168440001901103.
21. Payal Jain, Ashwini Kumar, Post buckling response of square laminates with a central circular/elliptical cutout, Composite Structures 65 (2004) 179–185.
22. Philippe H. Geubelle and Jeffrey S. Baylor, Impact-induced delamination of composites: a 2D simulation, Composites Part B 29B (1998) 589–602.
23. Reddy JN, Khdeir AA, Buckling and vibration of laminated composite plates using various plate theories. AIAA J 1989;27(12):1808-17.
24. Reddy, J. N., Large amplitude flexural vibration of layered composite plates with cutouts, J. Sound and Vibration, 83 (1982) 1-10.

25. Richard WC Campanelli & John J. Engblom, The effect of delaminations in graphite/PEEK composite plates on modal dynamic characteristics, Composite Structures 31 (1995) 195-202.
26. S.A.M. Ghannadpour, A. Najafi *, B. Mohammadi, On the buckling behaviour of cross-ply laminated composite plates due to circular/elliptical cutouts. Composite Structures 75 (2006) 3–6
27. Sasank Sekhar Hota, Payodhar Padhi, Vibration of plates with arbitrary shapes of cutouts, Journal of Sound and Vibration 302 (2007) 1030–1036.
28. T.-P. Chang, C.-Y. Hu & K.-C. Jane, Vibration Analysis of Delaminated Composite Plates under Axial Load, MECH. STRUCT. & MACH., 26(2), 195-21 8 (1998)
29. Todd O. Williams And Frank L. Addessio, A Dynamic Model For Laminated Plates With Delaminations, Int. J. Solids Structures VoL 35, Nos. 1-2, pp. 83-106, 199.
30. V. Anil, C. S. Upadhyay, N. G. R. Iyengar, Stability analysis of composite laminate with and without Rectangular cutout under biaxial loading. : Composite Structures 80 (2007) 92-104.
31. W.M. Ostachowicz , S. Kaczmarczyk, Vibrations of composite plate with SMA fibers in a gas stream with defects of the type of delamination, Composite Structures 54 (2001) 305-311.